UNIVERSITY OF CALIFORNIA, SAN DIEGO

The Role and Location of TAM Receptors in the Thymus

A Thesis submitted in partial satisfaction of the requirements of the degree
Masters of Science

in

Biology

by

Christopher M Mayer

Committee in charge

Professor Greg Lemke, Chair
Professor Elina Zúñiga, Co-Chair
Professor Aaron Coleman
Professor Cornelis Murre

The Thesis of Christopher M Mayer is approved and it is acceptable in quality and form for publication on microfilm and electronically:

_____

_____

_____
Co-Chair

_____
Chair

University of California, San Diego

2015

DEDICATION

I dedicate this to my family and friends who have shown continued love and support throughout my years of learning. I want to dedicate this thesis to everyone who has motivated and pushed me, even during the late hours of the night. Most importantly, I also want to dedicate my thesis to God because I know that I would not have been able to accomplish any of this without his help and guidance.

TABLE OF CONTENTS

LIST OF FIGURES

ACKNOWLEDGEMENTS

I would like to thank Worakls and N'to for making the time fly while I was analyzing thousands of images and writing my thesis sections. You both are extremely gifted.

My passion for science really began sophomore year of high school and I need to thank my chemistry teacher, Ms. Chaney-Aiello, for always answering my questions and cultivating a sense of curiosity for the sciences. I also want to thank Dr. Jim Baxter for solidifying my love for biology. Your classes and teaching style helped me see the beauty of biology. Additionally, I want to thank Dr. Joseph O'Connor and Dr. Aaron Coleman. Each of you impacted how I look at problems and this will be imperative for my future as a physician.

And most importantly, I would like to thank my advisor, Dr. Greg Lemke. His continued support and guidance throughout my years of research have better prepared me for my future. I am also thankful for the opportunity to be part of a lab that treats everyone like family. I also want to thank my mentor, Dr. Anna Zagórska. Her direction and insight have helped me become the researcher I am today.

ABSTRACT OF THE THESIS

The Role and Location of TAM Receptors in the Thymus

by

Christopher M Mayer

Master of Science in Biology

University of California-San Diego, 2015

Professor Greg Lemke, Chair

Professor Elina Zúñiga, Co-Chair

Little is understood about the genesis of autoimmune diseases caused by deficiencies in TAM receptors (Tyro3, Axl, Mer). One of the causes of autoimmunity could be defective thymic education. Our goal was to elucidate the localization and role of TAM receptors and their ligands within the thymus. We show that Axl and Mer, but not Tyro3, are expressed within the thymus. Through immunohistochemistry, we identify Axl and Mer expression primarily on macrophages in both the medulla and cortex. Using knockout mice, we show that Axl and Mer perform necessary but redundant roles in the elimination of basally accumulated apoptotic thymocytes. The absence of both receptors leads to immense apoptotic cell accumulation within thymic cortex and medulla.

These changes result in minor morphological defects as the weight but not the ratio of medulla to cortex was affected in the *Axl*$^{-/-}$*Mertk*$^{-/-}$ mice. We further use this model to instigate Axl dependence on Gas6 as a ligand in thymus. Additionally, we show that during acute thymocyte apoptosis, Mer but not Axl is critical in cellular clearance.

INTRODUCTION

The maintenance of the immune system is complex yet imperative for survival. Failure to properly maintain the immune system can either lead to susceptibility to infections or various autoimmune diseases (ADs). It is estimated that 23.5 million Americans have at least 1 of 24 diagnosable ADs (NIH). In comparison, cancer affects 15 million (American Cancer Society). Furthermore, AD accounts for $100 billion per year in direct health care costs compared to obesity, which costs $86 billion.

Vertebrates have an innate and adaptive immune system and the latter is comprised of humoral and cellular defenses. The thymus is a critical organ for generating the cellular defense of the adaptive immune system. The thymus is responsible for educating naïve thymocytes to properly defend against foreign antigens while ensuring they do not attack self in the process. Located above the heart, the thymus is a white organ consisting of two dorsoventrally adjacent oval lobes. The thymus is composed of two distinct regions, the cortex and medulla. Anatomically, the cortex is densely packed with the cells, while the cells in the medulla are more dispersed.

The thymus first receives pro-thymocytes from bone marrow and graduates fully functional CD4+ or CD8+ T cells. The pro-thymocytes first begin their journey in the junction between the cortex and medulla (Takahama, 2006). Traveling deeper into the cortex, the population first begins to divide and rearrange their T cell receptors (TCR). At this stage, the thymocytes are double negative (DN) for both CD4 and CD8 molecules. The β, γ and δ TCR subunits

are rearranged to determine if the cell will become an αβ or γδ T cell. Almost all thymocytes undergoing rearrangement are fated for the αβ T cell lineage (Ciofani et al., 2006). For the purposes of this paper, we will focus on the αβ T cell lineage. The next step for αβTCR-expressing DN thymocytes is to become double positive (DP) thymocytes (CD4+ and CD8+). This step is controlled through TCR-β recombination, as the recombination of the β gene locus is critical in forming a functional preTCR complex (Surh and Sprent, 1994).Thymocytes in this stage possess an apoptotic phenotype but with a viable preTCR, the thymocytes can avoid being phagocytosed and continue on the process to become a mature T cell (Haks et al., 1999; Mandal et al., 2005; Vollmer et al., 2000). Furthermore, successful creation of a functional preTCR will enable cellular expansion to occur for those cells. This is the first of two checkpoints that reside in the thymic cortex (Petrie and Zuniga-Pflucker, 2007). After passing this checkpoint, the thymocytes become DP (Szondy et al., 2012). The second checkpoint quickly follows once the α-chain rearranges and combines with the β-subunit. The TCR-αβ is tested on its ability to interact with major histocompatibility complex (MHC) expressed on cortical thymic epithelial cells (cTECs) (Speiser et al., 1989; Spits, 2002). If the TCR is specific for MHC-I, the T cell will become a $CD8^+$ SP T cell and if the TCR is specific for MHC-II, the T cell will become a $CD4^+$ SP T cell (Deftos et al., 2000; Robey and Fowlkes, 1994). If the TCR-MHC interaction is too strong, the T cell will undergo apoptosis through the process of negative selection (Palmer, 2003). If the TCR does not bind with enough affinity, the maturing thymocytes will not receive necessary signals to

continue through the education process and die of neglect. After the second checkpoint in the cortex, 95% of the thymocytes that have entered or appeared through clonal expansion have been marked for apoptosis and efficiently cleared by macrophages (Goldrath and Bevan, 1999). By completing the second checkpoint, the SP thymocytes migrate from the cortex to the medulla.

The third checkpoint examines the TCR affinity for self-antigens by having the maturing thymocytes randomly move within the medulla (Witt et al., 2005). Here, medullary thymic epithelial cells present an array of tissue-specific antigens (TSAs) through the Aire (Autoimmune regulator) transcription factor (Derbinski et al., 2001; Weinreich et al., 2011). T cells that recognize and show an affinity for TSAs will be eliminated through negative selection. It has been proposed that T cells undergoing negative selection move slower in the medulla and increase both contact-frequency and duration with dendritic cells (DCs) (Le Borgne et al., 2009). Cells that are negatively selected become apoptotic and are quickly cleared by thymic macrophages. This process removes the T cells that have the potential to cause peripheral autoimmunity. After 4-5 days, if the T cell has not been targeted for negative selection, the thymocytes will completely mature and emigrate from the thymus (McCaughtry et al., 2007).

Through thymic education, there are two checkpoints in the cortex and a final checkpoint in the medulla. At each checkpoint, apoptotic cells are quickly cleared by macrophages (Surh and Sprent, 1994; Wood, 1985). The ability for macrophages to clear apoptotic cells relies on the expression of phagocytic receptors. One major phagocytic receptor family is the TAM receptor tyrosine

kinase family, which derives its name from its three members: Tyro3, Axl and Mer. These receptors are expressed on professional phagocytes and have been shown to play a vital role in the homeostatic clearance of apoptotic cells (Lemke and Burstyn-Cohen, 2010). TAMs are expressed on professional phagocytes in the brain, testes, retina as well as other organs (Pierce and Keating, 2014). In order for the receptors to function they require circulating ligands - Protein S (ProS) and Gas6 (growth-arrest-specific 6)(Stitt et al., 1995; Varnum et al., 1995). Either ProS or Gas6 can activate Mer and Tyro3, while Axl is limited to Gas6 (Lew et al., 2014).

The TAM ligands are bimodal – they bind to the extracellular domain of the receptors and to exposed phosphatidylserine (PtdSer) on apoptotic cells. The binding of these ligands to PtdSer is a Ca^{2+}-dependent process and requires the vitamin K-dependent gamma-carboxylation of the glutamic acids on the ligands (Lemke and Rothlin, 2008). PtdSer is a structural lipid and one of the classic “eat-me” signals that mark cells for phagocytosis (Ravichandran, 2010). On living cells, PtdSer is confined to the inner leaflet of cell membrane through the activity of lipid flippases in the P4-ATPase family (van Meer et al., 2008). After the cell is signaled for apoptosis, scramblases, that are either Ca^{2+} or caspase-dependent, will relocate PtdSer so that it is exposed on the surface (Segawa and Nagata, 2015).

Beyond ligand specificity, TAMs further differ in their downstream function after phagocytosis. It is described *in vitro* that Mer performs a more basal phagocytic function, while Axl is more associated with proinflammatory settings

(Zagorska et al., 2014). Being that TAMs are crucial for the clearance of apoptotic cells, it would be expected that they are expressed and function in the thymus. Previous work has shown that Mer is expressed in the thymus and plays a critical role with the phagocytosis of apoptotic cells (Scott et al., 2001; Seitz et al., 2007). Additionally, Axl is highly expressed in epidermal DCs (Langerhans cells) and plays a crucial role in the phagocytosis of apoptotic cells suggesting that Axl may also be present on DCs within the thymus (Bauer et al., 2012). However, the expression of Axl and Tyro3 in the thymus has not been tested. Investigating the potential role of all three TAM receptors in the thymus is important because mice lacking Axl and Mer or lacking all three receptors (TAM tKO) develop spontaneous broad-spectrum autoimmune diseases.

The goal of our project was to first determine which TAM receptors were present in the thymus and if they were confined to specific regions and cell populations. Our next goal was to determine their role in phagocytic clearance of apoptotic thymocytes. We used TAM receptor knockout mice to analyze their thymic function both in basal conditions and after thymic insult. Finally we wanted to examine if there were gross anatomical changes within the thymus caused by the knockout of TAM receptors.

Materials and Methods

Materials

Mice

All mice were pure C57Bl/6 background. They were bred and housed within Animal Facilities at Salk Institute (La Jolla, CA). Mice were contained in a controlled environment under a 12-hour light/dark cycle. All experiments and maintenance for the mice was conducted under established guideline of the International Animal Care and Use Committee (IACUC). The *Tyro3*$^{-/-}$, *Axl*$^{-/-}$, *Mertk*$^{-/-}$ and *Axl*$^{-/-}$*Mertk*$^{-/-}$ mutants (Lu et al., 1999) and the *Gas6*$^{-/-}$ mutants (Angelillo-Scherrer et al., 2001) were previously described. Crossing *Mertk-/-* and *Gas6*$^{-/-}$ mice generated *Mertk*$^{-/-}$*Gas6*$^{-/-}$ mutants. All mice used ranged from 1 week to 12 weeks of age. For all experiments, mice were female with the exception of one male WT and *Mertk*$^{-/-}$ at the 3-week time point. Mice were randomly assorted into groups (three mice) for the DEX experiment. With all the experiments, investigators were not blinded to mouse genotype.

Antibodies

Antibodies used for colocalization and AC quantification: anti-Mer (R&D, polyclonal), anti-Mer (eBioscience; DS5MMER), anti-CD86 (Biolegend; P03), anti-MHCII (EMD Millipore; M5/114), anti-CD45R (B220) (Invitrogen; RM2600), anti-CD11b (Invitrogen; RM2800), anti-Ly6C (Biolegend; RB6-8C5), anti-F4/80 (PAQUI!!), anti-CD68 (AbDSerotec; MCA1957), anti-CD11c (eBioscience; N418), anti-MARCO (AbD Serotec; ed31), anti-CD169 (AbDSerotec; 3D6), anti-SIGN-R1

(serum, pAb), anti-cCasp-3 (Cell Signaling; D175), anti-Caspase-3 (Cell Signaling), anti-hProS 1 (R&D, pAb), anti-Gas6 (R&D, pAb).

Primary antibodies used for western blot analysis were anti-Axl (R&D, polyclonal), anti-Mer (R&D, polyclonal), anti-Tyro3 (antisera #5424, provided by Dr. Cary Lai), and anti-GAPDH (MAB374; 6C5).

Secondary antibodies used for western blot analysis were horseradish peroxidase–conjugated anti-goat (705-035-003; Jackson ImmunoResearch), anti-mouse (NA931V; GE Healthcare) and anti-rabbit (NA934V; GE Healthcare).

Secondary antibodies for immunohistochemistry were fluorophore-conjugated anti-goat (A-11055 (Life Technologies) or 705-166-147 (Jackson ImmunoResearch)) and anti-rat (712-606-153, 712-165-153 and 712-545-153; all from Jackson ImmunoResearch).

Methods—

Preparation of Thymic Sections

Thymus was harvested from mice sacrificed via 1.5 LPM of CO_2 followed by manual cervical dislocation. Mice were weighted immediately after cervical dislocation. The excised thymus was cleared from any blood during the procedure and immediately places in O.C.T (Tissue-Tek). In some cases, the thymus was weighed upon placement into O.C.T. The thymus was fresh frozen and cut into 11 μm thick sections on a Cryostat (H/I Bright). Sections were air-dried for 24 hours and then stored desiccated at -70 °C. Before staining, sections were fixed in ice-cold acetone for 3 minutes and then placed in PBS for 5

minutes. Sections were blocked with blocking buffer against the secondary antibody species for 2 hours (PBS with 0.1% Tween-20 (Sigma-Aldrich), 5% Normal Donkey Serum, 2% BSA-IgG Free and 0.02% Azide). Sections were washed once with 0.1% Tween-20 in PBS and incubated with primary antibodies diluted 1:100 in blocking buffer overnight at 4 °C. Sections were washed 5 times for 5 minutes each in PBS-0.1% Tween-20 and then incubated in the dark at room temperature with secondary antibodies diluted 1:400 in blocking buffer and 0.0025% Hoechst 33258 (ThermoFischer) (1:400) in blocking buffer. Secondary antibodies were spun down for 25 minutes at 15,000 rpm at 4 °C before staining to remove any aggregates. Sections were washed using the same protocol and then placed in PBS. The slides were mounted using Fluoromount-G (SouthernBiotech), sealed with clear nail polish and stored in the dark at 4 °C.

Apoptotic Cell Imaging

Thymic images were taken with Zeiss LSM 700 Confocal microscope. 20x magnification was chosen to capture sufficient structure and area without compromising identification of individual cell. Images were focused to obtain the best signal of cCasp3 throughout the entire image. Imaging parameters were conserved throughout all images.

Determining Thymic Regions within Sections

Thymic sections were analyzed using ImageJ. CD86 and Hoechst 33258 were both used to identify the medulla from the cortex in the thymus. CD86 staining strongly marked the medulla of the thymus. Hoechst differentiated the

medulla from the cortex because the cortex is more densely packed with cells compared to the medulla. CD86 staining was used first and Hoechst was used secondly as a confirmation of the CD86 staining. The regions were drawn using the Polygon Selections tool in ImageJ.

Basal Apoptotic Cell Quantification and Thymic Region Determination

Images taken on the confocal microscope were analyzed using ImageJ. Each image had the medulla and cortex portion identified as described above. The cortex and medulla were analyzed separately for apoptotic cell accumulation. The area of each region was quantified using the Measure function. Images were channel split and the cCasp3 split channel's threshold was modified in B&W to a lower and upper limit of 49 and 255, respectively. A single apoptotic cell signal was estimated to range between 6 - 149 μm^2, based on manual counting. Signals equal or larger than 150 μm^2 were considered cell doublets. There were no circularity restrictions. Each region was counted using the Analyze Particle tool and set to the parameters that were determined through manual counting. Each genotype was analyzed with at least 3 mice per age. Almost all the mice were females to control for potential variations between sexes. Each mouse thymus had 3 sections analyzed, spaced over 100 μm apart. Each section had 5 images taken, with each image varying the amount of medulla and cortex to ensure representative coverage. Within each section, the apoptotic cells were summed separately in cortex and medulla. This sum was divided by the counted area and presented as a number of AC per mm^2. For

each mouse all the sections were averaged together. For each genotype, the mean and S.E.M were presented.

Dexamethasone Injections

Mice at 12 weeks of age were intraperitoneally injected with Dexamethasone sodium phosphate (Bimeda) at 0.2 mg per 25 g as described before (Scott et al., 2001). Injections were performed in the afternoon. Whole thymus was removed from the mice 24h later and was fresh frozen in O.C.T. Dexamethasone-treated thymus underwent same preparation protocol as other thymus.

Dexamethasone Injection Apoptotic Cell Quantification

Dexamethasone-injected thymus followed the same slide preparations, imaging procedure, and region determination as other thymuses. Quantification of apoptotic cells used ImageJ software. Due to large AC accumulation, counting individual cells was not feasible. The AC area was calculated instead. Each image was channel split and had the threshold conformed to the same parameters as in the basal apoptotic cell accumulation method. The cumulative apoptotic cell area was analyzed using the Analyze Particles tool. This area was divided by the total area of each thymic region. Each genotype had at least 3 mice per age. Each mouse thymus had 3 sections analyzed, spaced over 100 μm apart. Each section had 5 images taken, with each image varying the amount of medulla and cortex to ensure representative coverage.

Hematoxylin & Eosin Staining

Thymic sections were brought to room temperature from -70 °C in storage. Slides were first placed in Mayer's Hemotoxylin (Sigma-Aldrich) for five minutes. Slides were then transferred to 37 °C tap water for five minutes. After, the slides were placed in EosinY, Alcoholic (Sigma-Aldrich) for 60 seconds and then immediately transferred to 100% EtOH (Sigma-Aldrich) for 60 seconds. The sides were then transferred into Histo-Clear (National Diagnostics) for five minutes. VectaMount (Vector) was applied to mount the slides. Slides were stored in the dark at room temperature.

Hematoxylin & Eosin Area Analysis

Thymic sections (stained with Hematoxylin and Eosin) were analyzed on the Olympus BX40 microscope. Images were taken at 4x and manually stitched together using Adobe Illustrator. The area was assessed using the Polygon Tool from ImageJ. Pink regions denoted the medulla and the dark purple regions denote the cortex.

Western Blotting

Excised thymus was cut in half with a razor blade and snap frozen in liquid nitrogen. Samples were lysed on ice in a lysis buffer containing 50mM Tris-HCl pH 7.5, 1mM EGTA, 1mM EDTA, 1% Triton X-100, 0.27 M sucrose, 0.1% β-mercaptoethanol, and protease and phosphatase inhibitors (Roche). Samples were examined and standardized for protein concentration through Bradford Assay (Bio-Rad). Equal amounts (20 µg) of protein were loaded per well with

LDS Sample Buffer (Invitrogen). Samples were separated by electrophoresis on 4-12% Bis-Tris polyacrylamide gels at 90V (Novex, Life Technologies). Samples were transferred to PVDF membranes (Millipore) for 90 minutes at 200mA. Membranes were analyzed via Ponceau S staining (Sigma-Aldrich) and then washed for 5 minutes with dI water. Membranes were blocked with 5% BSA (American Bioanalytic) in TBS with 0.25% Tween-20 for 90 minutes. Membranes were then incubated with primary antibody diluted 1:1000 in blocking buffer overnight at 4°C and then washed 5 times with TBS-tween20 (0.25%) for 5 minutes each time on a rocker. Secondary antibody was added 1:5000 into 5% non-fat dehydrated milk in TBS-tween20 (0.25%) and incubated 90 minutes at room temperature. Membranes then followed the same wash pattern as after primary antibody. After a fifth wash, membranes were briefly washed in TBS. Membranes were incubated in enhanced chemiluminescence reagent (ECL) and signal was detected on autoradiography films (Carestream and Denville Scientific Inc).

Graphical Analysis and Statistics

Data was analyzed using GraphPad Prism 6 software (San Diego, CA). Statistical significance on all bar graphs used unpaired t-tests, assuming that both populations have the same variation. We also assumed Gaussian distribution for the analysis. P value was calculated through two-tail analysis. $P \leq 0.05$ was defined as statistically significant (*). $P \leq 0.01$ was denoted as (**). $P \leq 0.001$ was denoted as (***).

In order to determine if there was a correlation between body weight and thymic weight, we analyzed the Pearson correlation coefficient (r).

Results

Determining TAM receptor expression in Thymus

To ascertain the expression of TAM receptors in the thymus, we analyzed thymic cell lysates from WT, *Tyro3*$^{-/-}$, *Axl*$^{-/-}$, *Mertk*$^{-/-}$ and *Gas6*$^{-/-}$ mice. Analysis confirmed that Axl and Mer but not Tyro3 were expressed in the thymus (Figure 1). Tyro3 expression was not detected in any of the samples (data not shown). Additionally, we blotted for Gas6, a common ligand for both Axl and Mer. Gas6 presence in *Axl*$^{-/-}$ thymus was reduced compared to other genotypes (Figure 1), which was expected because Gas6 is prebound to Axl in many tissues. We were not able to detect ProS through Western blot analysis (data not shown).

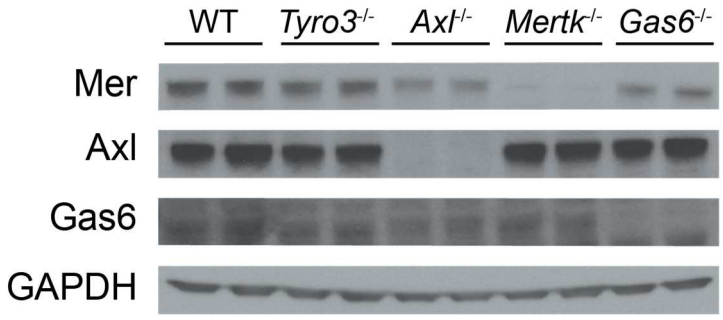

Figure 1. Analysis of TAM Receptor and Ligand Presence in Thymus. Western blot analysis was performed on 20 µg of thymic lysates from WT (wild-type), *Tyro3*$^{-/-}$, *Axl*$^{-/-}$, *Mertk*$^{-/-}$ and *Gas6*$^{-/-}$ mice. Duplicates are two separate mice for each genotype. GAPDH was used as a loading control.

Since Axl and Mer were the only TAMs detected by Western blot analysis, we performed further studies focusing on the thymic role of Axl and Mer.

Determining the Thymic region that has Axl and/or Mer-expressing cells

To investigate the role of Axl and Mer within the thymus, colocalization assays were conducted to determine the cellular populations that expressed

either or both of the receptors of interest. Nine different cellular markers were chosen that distinguished cell populations within the thymic cortex and medulla. Three additional new markers were tested because of their biological importance within other organs responsible for the efficient clearance of apoptotic cells.

To localize Axl and Mer within cortex or medulla, thymic sections from WT 4-week-old female mice were stained with anti-Axl and anti-Mer antibodies. The slides were also costained with Hoechst and CD86. Hoechst, a nucleic acid dye, was used to differentiate regions in thymus based on cell density. The dense and less dense regions are the cortex and medulla, respectively. To confirm the regional identification by Hoechst, CD86 (also known as B7-2) was also used (Figure 2A). CD86 is a plasma membrane protein on antigen presenting cells used to provide costimulatory signaling to thymocytes and is preferentially localized in the medulla (Figure 2A) (Damoiseaux et al., 1998; Degermann et al., 1994).

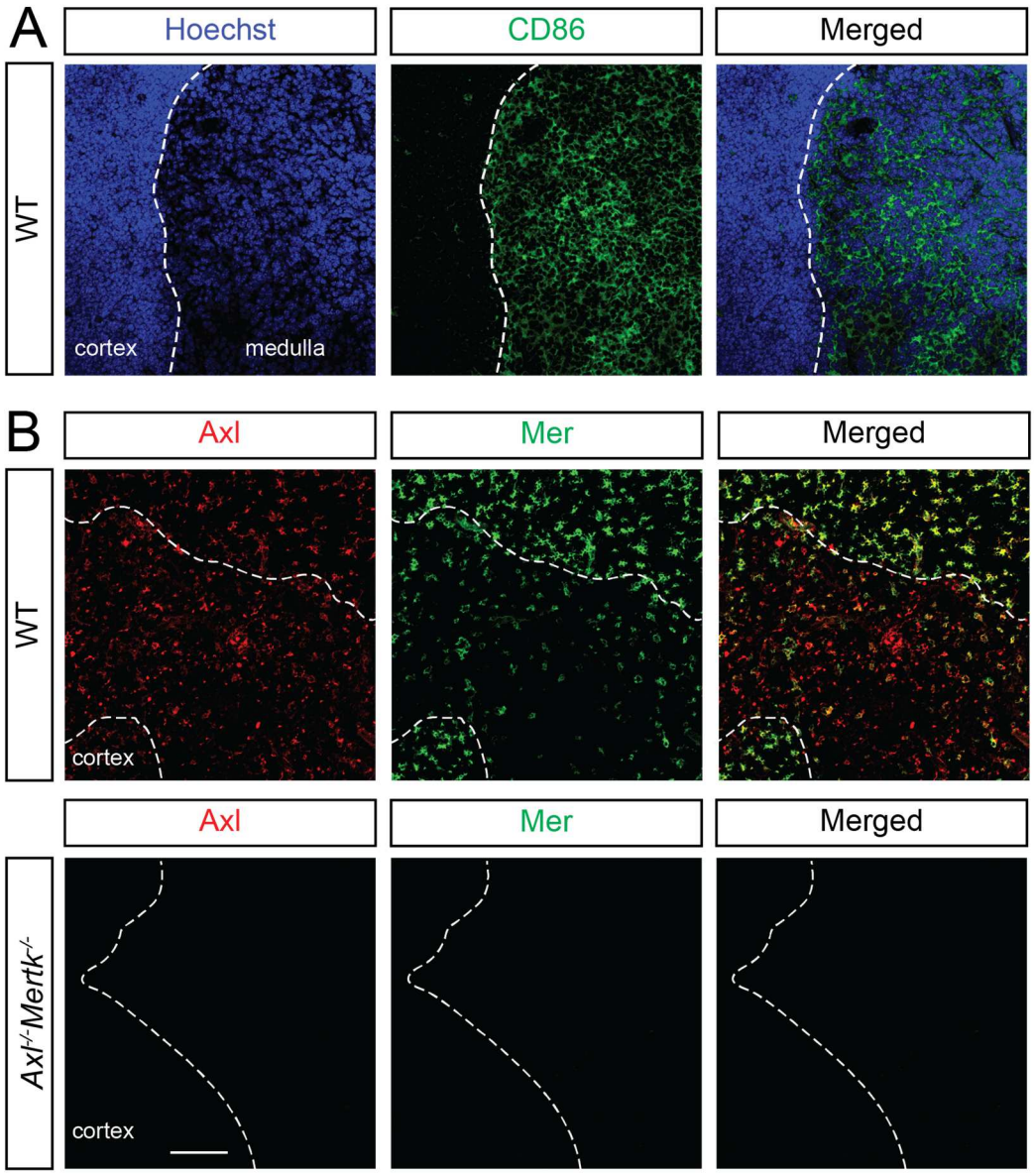

Figure 2. Regional Segregation Confirmation and TAM Receptor Colocalization. Thymic sections analyzed through immunohistochemistry for Axl, Mer and CD86. Scale bar,100 μm.

We showed that Axl and Mer were expressed both in the cortex and medulla. While Axl was equally expressed on cells in the medulla and cortex, Mer was expressed on fewer cells within the medulla (Figure 2B). All Mer^+ cells were also Axl^+. In addition, there was a subpopulation of cells in the medulla that were only Axl^+ with a rounded morphology (Figure 2B). The morphology of the

unique Axl^+ subpopulation was circular, with a dense signal. The specificity of Axl and Mer antibodies was confirmed by staining *Axl*$^{-/-}$*Mertk*$^{-/-}$ thymic sections (Figure 2B).

Lack of Axl colocalization with MHCII, B220, CD11b and Ly6C

After confirming the presence of Axl and Mer within the thymus, we next wanted to locate which cells expressed our receptors of interest. As most of the cells are both Axl and Mer positive, we used Axl in further colocalization studies. We used antibodies against MHCII (1-A/I-E), B cell marker B220 (also known as CD45R), macrophage marker CD11b, and monocyte marker Ly6c (also known as Gr1) (Geissmann et al., 2003; Riedinger et al., 1997). MHCII expression was localized in the medulla on mTECs and did not colocalize with Axl^+ cells. $CD11b^+$ positive macrophages and $B220^+$ B cells primarily resided in the medulla and were also Axl^-. The few $Ly6C^+$ monocytes in the thymus were mostly contained in the medulla and were also Axl^- (Figure 3). We established that Axl is not present on mTECs, $CD11b^+$ macrophages, monocytes or B cells in the thymus.

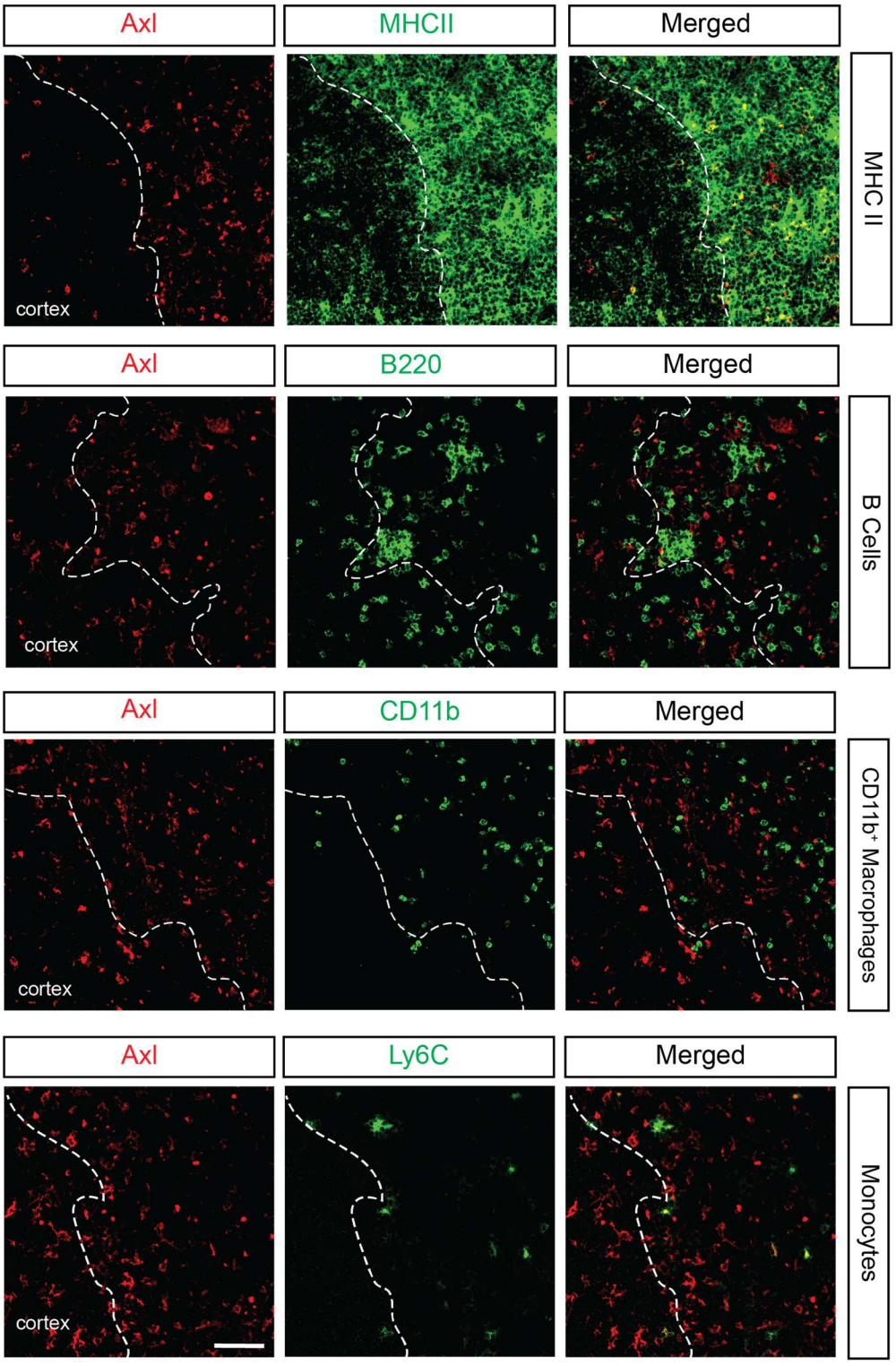

Figure 3. Thymic Cell Populations that do not Colocalize with Axl. Thymic sections were analyzed through immunohistochemistry for MHCII, B220, CD11b and Ly6C. Scale bar,100 μm.

Axl Colocalization with F4/80, CD68, and CD11c

We next investigated whether F4/80 (also known as Ly71 and EMR1) was coexpressed with Axl. F4/80 is a known marker for mature murine macrophages (Hirsch et al., 1981; Morris et al., 1991). F4/80 antigen is a glycoprotein and its expression is increased when macrophages are activated. $F4/80^+$ cells were located both in the cortex and medulla, with increasing density closer to the CMJ, and were all Axl^+ (Figure 4). However, F4/80 was on most, but not all, Axl^+ cells. Another tissue resident macrophage marker is CD68 (Murray and Wynn, 2011). CD68 also colocalized with Axl in the medulla and cortex (Figure 4). F4/80 and CD68 colocalization assays established Axl, and in extrapolation Mer, are mostly expressed by tissue-resident macrophages in the medulla and cortex of the thymus.

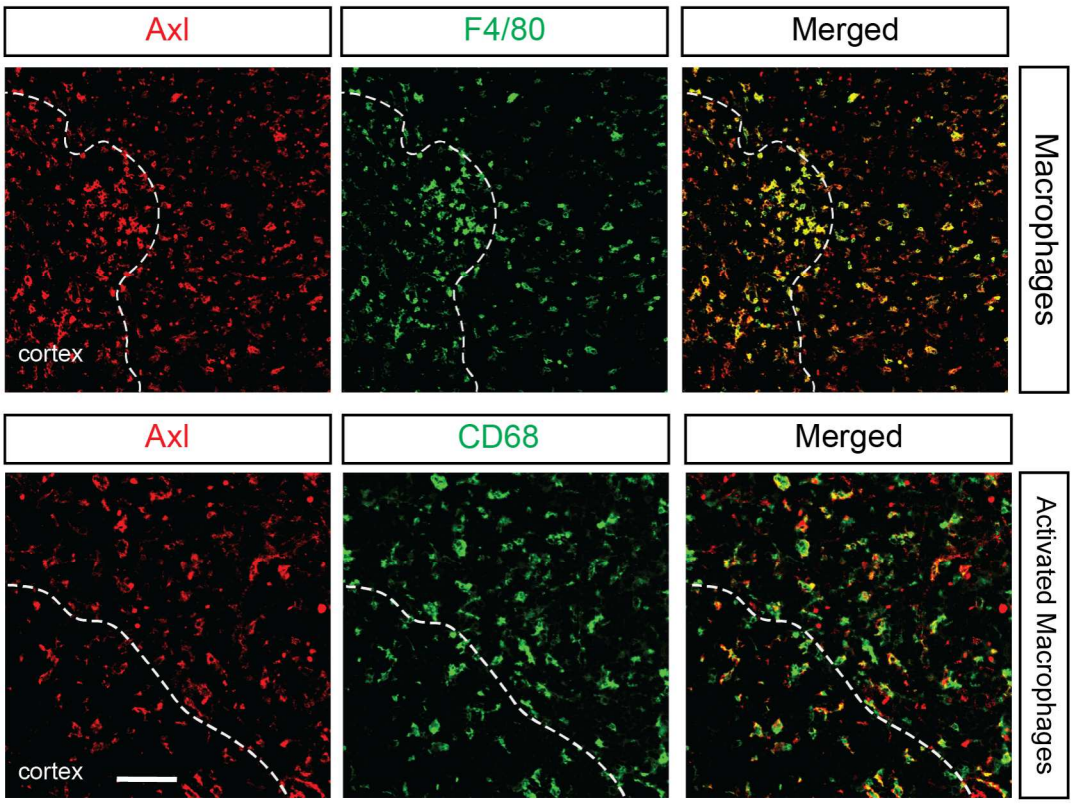

Figure 4. Axl Colocalization with Thymic Macrophage populations. Thymic sections were analyzed through immunohistochemistry for F4/80 and CD68. Scale bar,100 μm.

To investigate whether Axl was also expressed on DCs in the thymus, we used the DC marker, CD11c (Murray and Wynn, 2011; Wu and Shortman, 2005). Thymic DCs localize to the medulla and CMJ of the thymus (Ardavin, 1997). A fraction of $CD11c^+$ cells within the medulla coexpressed Axl (Figure 5). Additionally, there is a sparse $CD11c^+$ population in the cortex that does not express Axl. Therefore Axl is expressed on certain subsets of DCs within the medulla and CMJ.

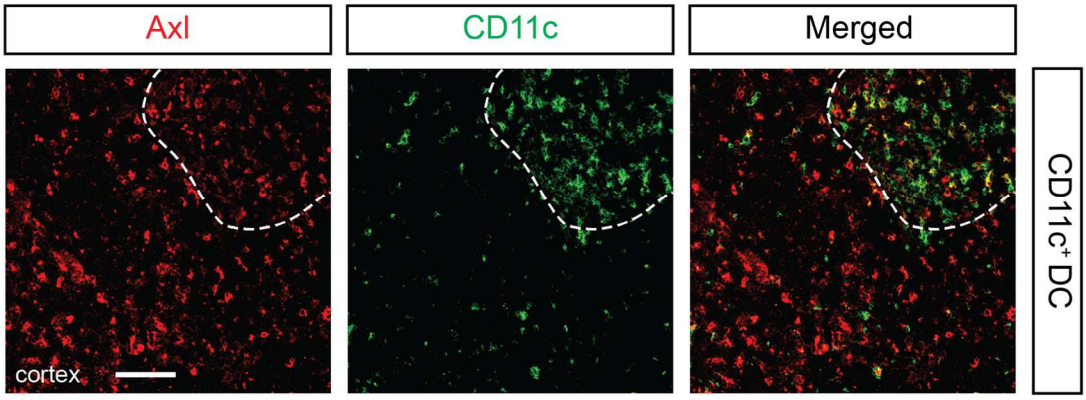

Figure 5. Axl Colocalization with Thymic DC Populations. Thymic sections were analyzed through immunohistochemistry for CD11c. Scale bar,100 µm.

Additional Marker Analysis in Thymus

To further elucidate thymic cell populations expressing Axl, we used additional cell markers that are specific to immune cell population in other lymphoid organs. These experiments test for the presence of these receptors in the thymus as well as their colocalization with Axl. The three additional markers used were MARCO (Macrophage receptor with collagenous structure), CD169 (also known as Siglec-1 and siloadhesin) and SIGN-R1 (SIGN-related 1).

MARCO has been described as a macrophage-specific receptor, preferentially expressed in both the splenic marginal zone and lymph nodes (Kraal et al., 2000). We establish that MARCO expression in the thymus is primarily in the cortex with a smaller subpopulation in the CMJ. Axl is expressed on almost all MARCO$^+$ cortex and CMJ populations (Figure 6).

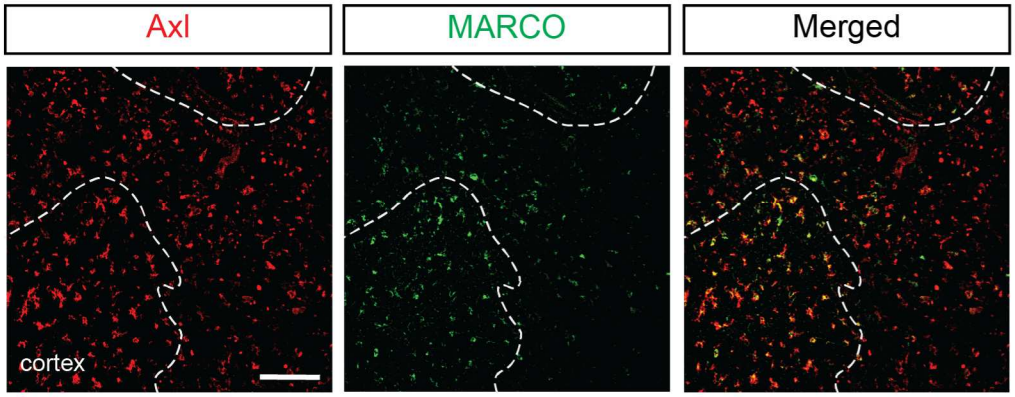

Figure 6. MARCO Expression and Colocalization in Thymus. Thymic sections were analyzed through immunohistochemistry for MARCO. Scale bar,100 μm.

CD169 is expressed on metallophilic macrophages within the spleen (Bernhard et al., 2015; Martinez-Pomares and Gordon, 2012). It has not been previously shown that $CD169^+$ populations existed in the thymus. Within the thymus, $CD169^+$ populations resided in the cortex and CMJ. All $CD169^+$ populations in the cortex coexpressed Axl. A subset of $CD169^+$ cells in the medulla possessed a rounded morphology and did not express Axl (Figure 7).

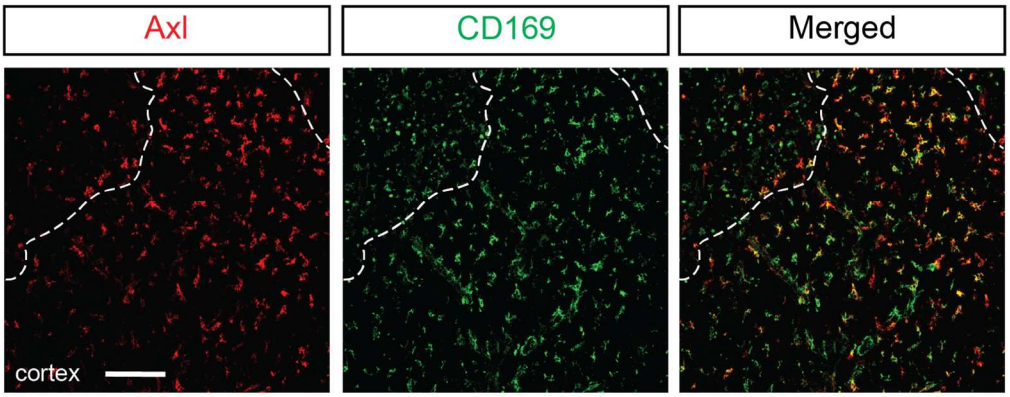

Figure 7. CD169 Expression and Colocalization in Thymus. Thymic sections were analyzed through immunohistochemistry for CD169. Scale bar,100 μm.

SIGN-R1 was the third marker used to analyze immune cell populations that have not been described in the thymus. SIGN-R1 is expressed by marginal

zone macrophages (MZM) in spleen as well as peritoneal macrophages (Kang et al., 2003; Koppel et al., 2005). Within the thymus, there was no expression of SIGN-R1 (Figure 8).

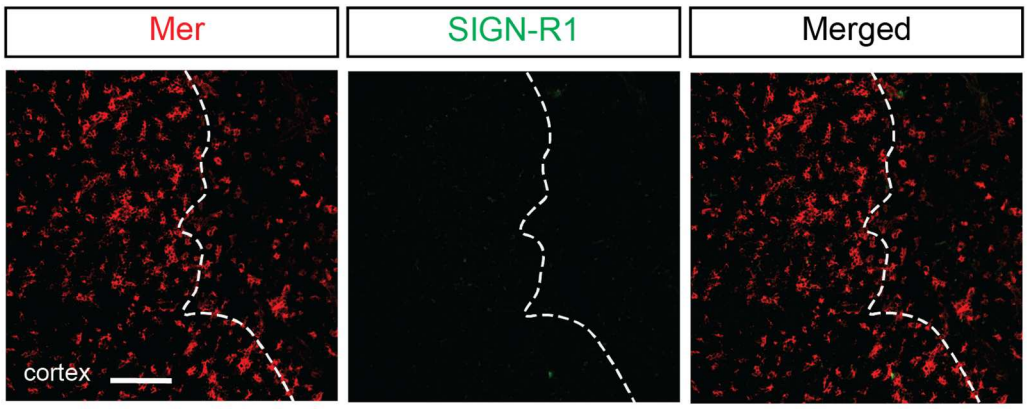

Figure 8. SignR1 Expression and Colocalization in Thymus. Thymic sections were analyzed through immunohistochemistry for SIGN-R1. Scale bar,100 μm.

We documented, for the first time, expression of MARCO and CD169 on cortical and CMJ macrophages in the thymus and showed that Axl is expressed by this population. In summary, Axl and Mer are expressed in the cortex and CMJ on $F4/80^{+}CD68^{+}MARCO^{+}CD169^{+}$ macrophages and in the medulla on $F4/80^{+}CD68^{+}$ macrophages. In addition, there is a small population of $Axl^{+}Mer^{-}$ $F4/80^{-}CD11c^{+}$ DCs in the medulla.

Apoptotic Cell Accumulation in Thymus

Given that our data and earlier results demonstrated that Axl and, by association, Mer expression was primarily on macrophages, we wanted to determine the role of these receptors in the thymus. As TAM receptors are involved in the clearance of apoptotic cells (ACs), we first used Western blot to

analyze levels of cleaved Caspase 3 (cCasp3) in thymus of WT and TAM receptor knockout mice (Figure 9). cCasp3 has been described as an early-stage marker for cellular apoptosis (Porter and Janicke, 1999). While all genotype possessed an equal amount of Caspase-3 (Casp3), cCasp3 was significantly increased in *Axl*$^{-/-}$*Mertk*$^{-/-}$ genotype (Figure 9).

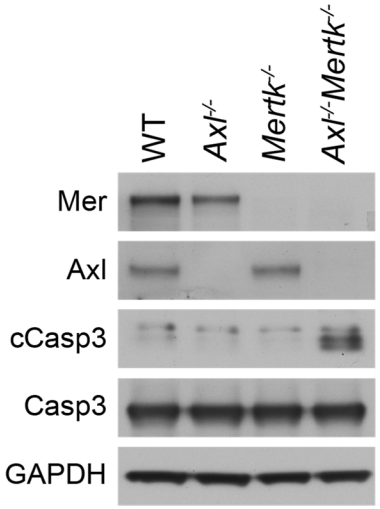

Figure 9. Increased cCasp3 Levels in *Axl*$^{-/-}$*Mertk*$^{-/-}$ Thymus. Thymic lysate from WT, *Axl*$^{-/-}$, *Mertk*$^{-/-}$ and *Axl*$^{-/-}$*Mertk*$^{-/-}$ mice were analyzed through Western blot for Mer, Axl, cCasp3 and total Casp3 protein level. 20 µg of thymic lysate was loaded per lane. GAPDH was used as a loading control

High levels of cCasp3 indicated accumulation of ACs specifically in *Axl*$^{-/-}$ *Mertk*$^{-/-}$. We next wanted to determine localization of ACs throughout the *Axl*$^{-/-}$ *Mertk*$^{-/-}$ thymus. Whole-section thymic images stained with cCasp3 and CD86 were tiled together for complete visualization. The tiled imaged showed that cCasp3 was primarily located in the cortex region of *Axl*$^{-/-}$*Mertk*$^{-/-}$ mice (Figure 10). Additionally, cCasp3 signal was strongest in the subcapsular zone of cortex, which is located around the periphery of the organ.

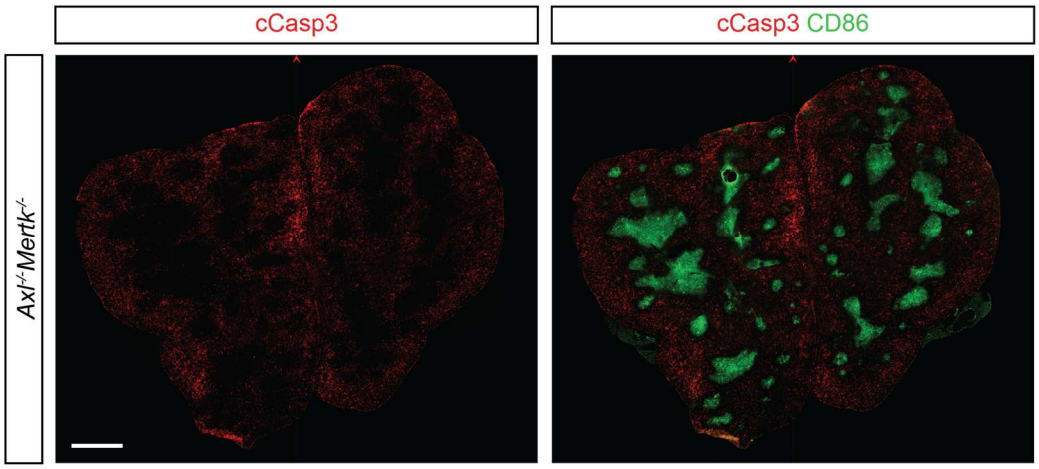

Figure 10. Tiled Image of *Axl*$^{-/-}$*Mertk*$^{-/-}$ Thymus. Tiled image of whole thymus stained with cCasp3 and CD86. Scale bar, 1 mm.

To further characterize and quantify the special and temporal distribution of AC accumulation we used cCasp3 immunohistochemistry in WT, *Axl*$^{-/-}$, *Mertk*$^{-/-}$, *Axl*$^{-/-}$*Mertk*$^{-/-}$ mice at 2, 3, 4, and 12 weeks of age. Since murine thymus is fully matured at 3-4 weeks and involution begins at 6 weeks, the 12-week-old animals were analyzed to monitor thymic involution. ACs were counted in both medulla and cortex, which were differentiated through Hoechst and CD86 signal.

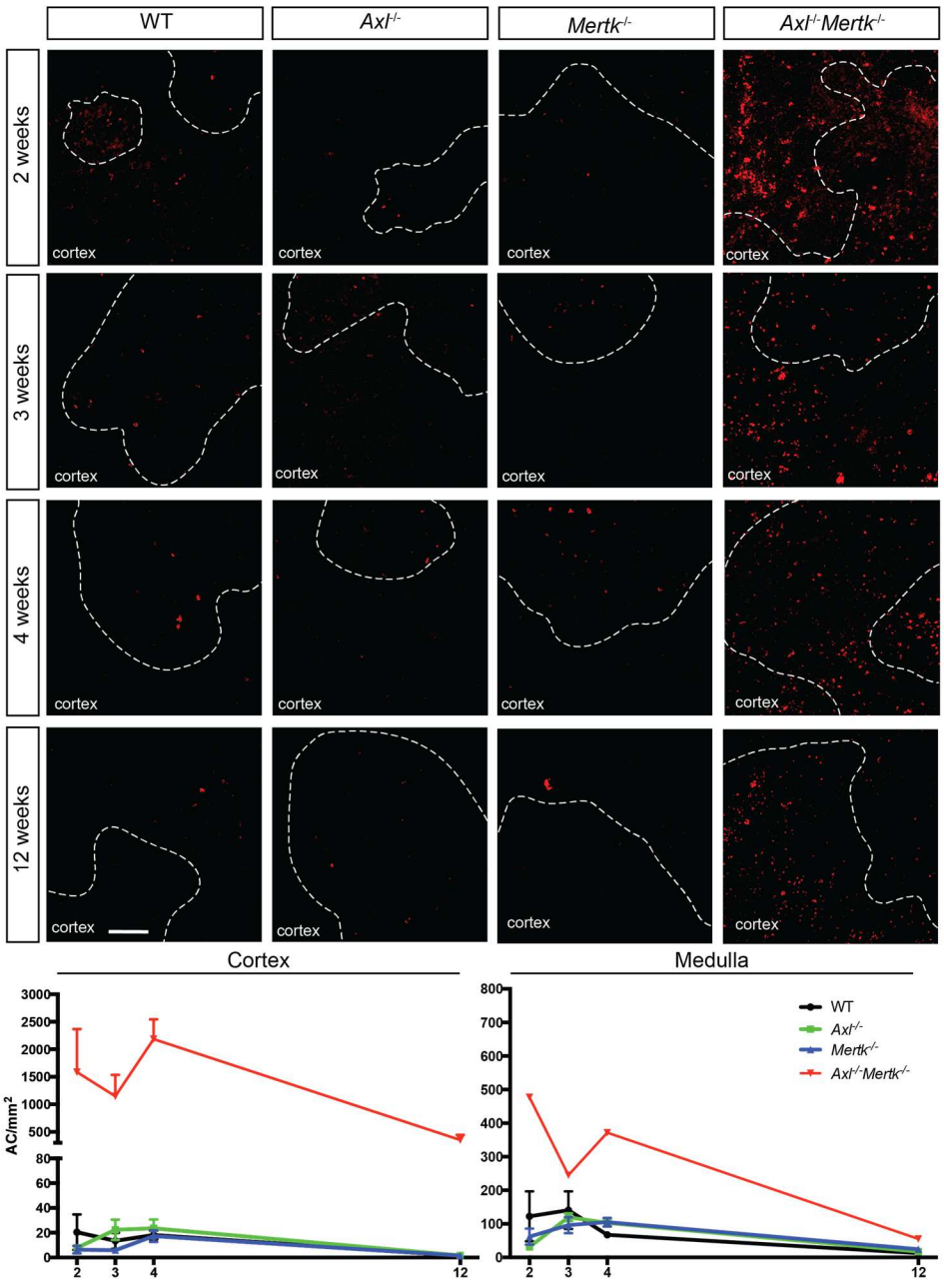

Figure 11. Immunohistochemistry and Analysis of Mouse Thymuses. Thymuses from WT and KO mice at indicated age were analyzed through immunohistochemistry for cCasp3. Representative images for each genotype and time point are displayed. Scale bar,100 μm. Graphs below show mean number of AC/mm^2. All points are averaged from n = 3 or 4. 12-week-old data is averaged from n=2. All error bars are SEM.

Images in Figure 11 show representative cCasp3 staining in thymuses of WT, *Axl*$^{-/-}$, *Mertk*$^{-/-}$, *Axl*$^{-/-}$*Mertk*$^{-/-}$ mice at 2, 3, 4, and 12 weeks of age.

Quantification of AC accumulation was done separately for cortex and medulla and is presented on the graphs below the images. 2 and 3-week-old mice show minor variations in AC accumulation between WT, *Axl*$^{-/-}$ *and Mertk*$^{-/-}$ thymuses, with higher number of ACs in the medulla compared to the cortex. At the same time points, *Axl*$^{-/-}$*Mertk*$^{-/-}$ have strongly increased AC accumulation in the medulla and cortex when compared to other genotypes. Furthermore, the accumulation is higher in the cortex than medulla for the *Axl*$^{-/-}$*Mertk*$^{-/-}$ mice (Figure 11). For all genotypes, the post-involution AC accumulation decreased in both the medulla and cortex (Figure 11). Similarly to the pre-involution thymus, the overall AC accumulation for WT was greater in the medulla than cortex. *Axl*$^{-/-}$ and *Mertk*$^{-/-}$ AC accumulation and location was similar to WT. Though *Axl*$^{-/-}$*Mertk*$^{-/-}$ had fewer accumulated ACs, there was still an increase compared to other genotypes. Like in the earlier time points, accumulation of ACs was dominant in the cortex (Figure 11).

Our most extensive analysis was performed for 4-week-old mice, which is a peak of thymic education. At 4 weeks of age, there was significant increase in the medullary AC accumulation for *Axl*$^{-/-}$ (P=0.0213), *Mertk*$^{-/-}$ (P=0.0250), compared to WT. In the cortex, there was no difference in AC accumulation for both *Axl*$^{-/-}$ and *Mertk*$^{-/-}$, compared to WT (Figure 12).

As for the 2 and 3-week-old mice, *Axl*$^{-/-}$*Mertk*$^{-/-}$ showed a much higher accumulation of ACs both in the cortex and medulla, when compared to WT (Figure 12). *Axl*$^{-/-}$*Mertk*$^{-/-}$ medullas had a 5-fold increase in ACs compared to WT

medullas (P=0.0161), whereas the cortexes had over 100-fold increase in ACs as compared to WT cortexes (P=0.0032).

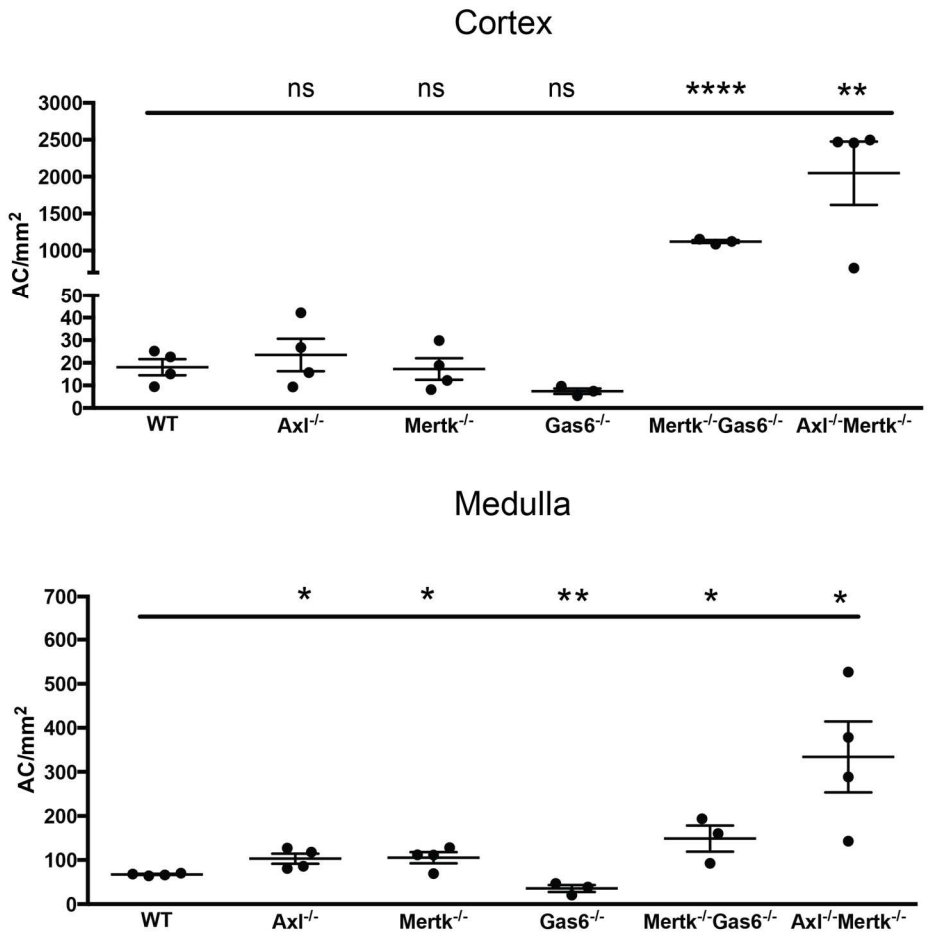

Figure 12. Basal 4-week-old AC Accumulation in Different Genotypes. Thymuses were analyzed through immunohistochemistry for cCasp3. WT, *Axl*$^{-/-}$, and *Mertk*$^{-/-}$ were averaged from n=4. *Mertk*$^{-/-}$*Gas6*$^{-/-}$ and *Axl*$^{-/-}$*Mertk*$^{-/-}$ were averaged from n=3. Each point represents one mouse. Significance was compared to WT. *P < 0.05; **P < 0.01; ****P < 0.0001; No significance, ns. All error bars are SEM.

Analysis of Gas6$^{-/-}$ and Mertk-/-Gas6-/- phenotype

Additionally, *Gas6$^{-/-}$* and *Mertk$^{-/-}$Gas6$^{-/-}$* were analyzed in 4-week-old mice. If Gas6 is the only ligand for Axl, then *Gas6$^{-/-}$* mice should phenocopy *Axl$^{-/-}$* mice, while *Mertk$^{-/-}$Gas6$^{-/-}$* mice should replicate the AC accumulation in *Axl$^{-/-}$Mertk$^{-/-}$* mice as the absence of Gas6 should completely inhibit Axl activation. When compared to WT, *Gas6$^{-/-}$* accumulated fewer ACs in the medulla (P=0.0051) but similar amount of ACs in the cortex. AC accumulation in *Gas6$^{-/-}$* thymic medulla had 3-fold fewer cells compared to *Axl$^{-/-}$* medulla (P=0.0064).

Analyzing 4-week-old thymuses in *Axl$^{-/-}$Mertk$^{-/-}$* and *Mertk$^{-/-}$Gas6$^{-/-}$* showed that both genotypes had increased accumulation of apoptotic cells in the cortex and medulla compared to WT (Figure 13). Both genotypes also shared a much greater accumulation of ACs in the cortex compared to medulla (Figure 12).

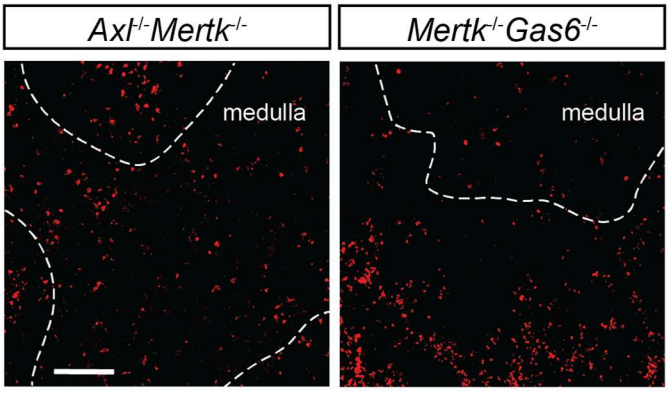

Figure 13. Representative Images of *Axl$^{-/-}$Mertk$^{-/-}$* and *Mertk$^{-/-}$Gas6$^{-/-}$* Thymus. Thymuses were analyzed through immunohistochemistry for cCasp3. Representative images are averaged from over 45 individual images. Scale bar,100 μm.

Interestingly, these two genotypes slightly but significantly differed with the AC accumulation in the cortex. *Axl$^{-/-}$Mertk$^{-/-}$* thymus accumulated over 2-fold more ACs when compared to *Mertk$^{-/-}$Gas6$^{-/-}$*. This result, together with the observation

that *Gas6*$^{-/-}$ and *Axl*$^{-/-}$ did not phenocopy AC accumulation in the medulla, suggested the removal of Gas6 ligand does not give exactly the same result as the removal of the receptor.

TAM Compensation Analysis

In WT thymus, Tyro3 expression was undetected by Western blot analysis (Figure 1) and by immunohistochemistry (data not shown). However, it was still possible that Tyro3 expression was induced in the thymuses of *Axl*$^{-/-}$, *Mertk*$^{-/-}$ or *Gas6*$^{-/-}$. Furthermore, it might be possible that *Axl*$^{-/-}$ mice could increase Mer expression or that *Mertk*$^{-/-}$ mice increase Axl expression, which could play a compensatory role in the phagocytosis of ACs. However, Western blot analysis showed no expression of Tyro3 in any of the genotypes. When looking for TAM receptor compensation, we established that there is no increase in either Axl or Mer expression among any of the genotypes. Furthermore, we noticed that Mer expression in thymus was actually slightly reduced in *Axl*$^{-/-}$ mice (Figure 1; Figure 9). In regards to *Gas6*$^{-/-}$ thymus, there was no detection of Tyro3 or any increased expression of Mer or Axl.

Role of Axl and Mer in Thymic AC clearance after Dexamethasone Injection

Our results showed that both Axl and Mer can perform apoptotic thymocyte clearance in basal conditions. We next wanted to understand the roles

of Axl and Mer when the thymus was additionally challenged through induction of thymocyte apoptosis. This would provide more insight into the capabilities and function of each TAM receptor. Dexamethasone (DEX) induces apoptosis of murine DP thymocytes (Purton et al., 2004; Tosa et al., 2003). 12-week-old WT, *Axl*$^{-/-}$, *Mertk*$^{-/-}$, and *Axl*$^{-/-}$*Mertk*$^{-/-}$ mice were injected IP with DEX at 0.2mg/25g, 24h before analysis. The thymic sections were analyzed for apoptotic cell accumulation. Since the degree of AC accumulation was so great for DEX-treated mice, the AC area was measured to compare the animals instead of the counting method used previously in the basal conditions (see methods). In DEX-treated WT and *Axl*$^{-/-}$ thymuses, there was no increase in the AC area in the medulla or cortex. However, *Mertk*$^{-/-}$ thymus showed 700 and almost 6,000-fold increase in AC area within the medulla and cortex, respectively. The *Axl*$^{-/-}$*Mertk*$^{-/-}$ showed similar AC accumulation as *Mertk*$^{-/-}$, with greater than 800 and 8,500-fold increase in medulla and cortex, respectively (Figure 14). There was no significant difference in the AC accumulation in either the medulla or cortex of DEX-treated *Axl*$^{-/-}$*Mertk*$^{-/-}$ thymuses when compared to *Mertk*$^{-/-}$ thymuses. These results indicated that after DEX injection, Mer was solely responsible for the clearance of apoptotic thymocytes, which was consistent with previous reports (Scott et al., 2001).

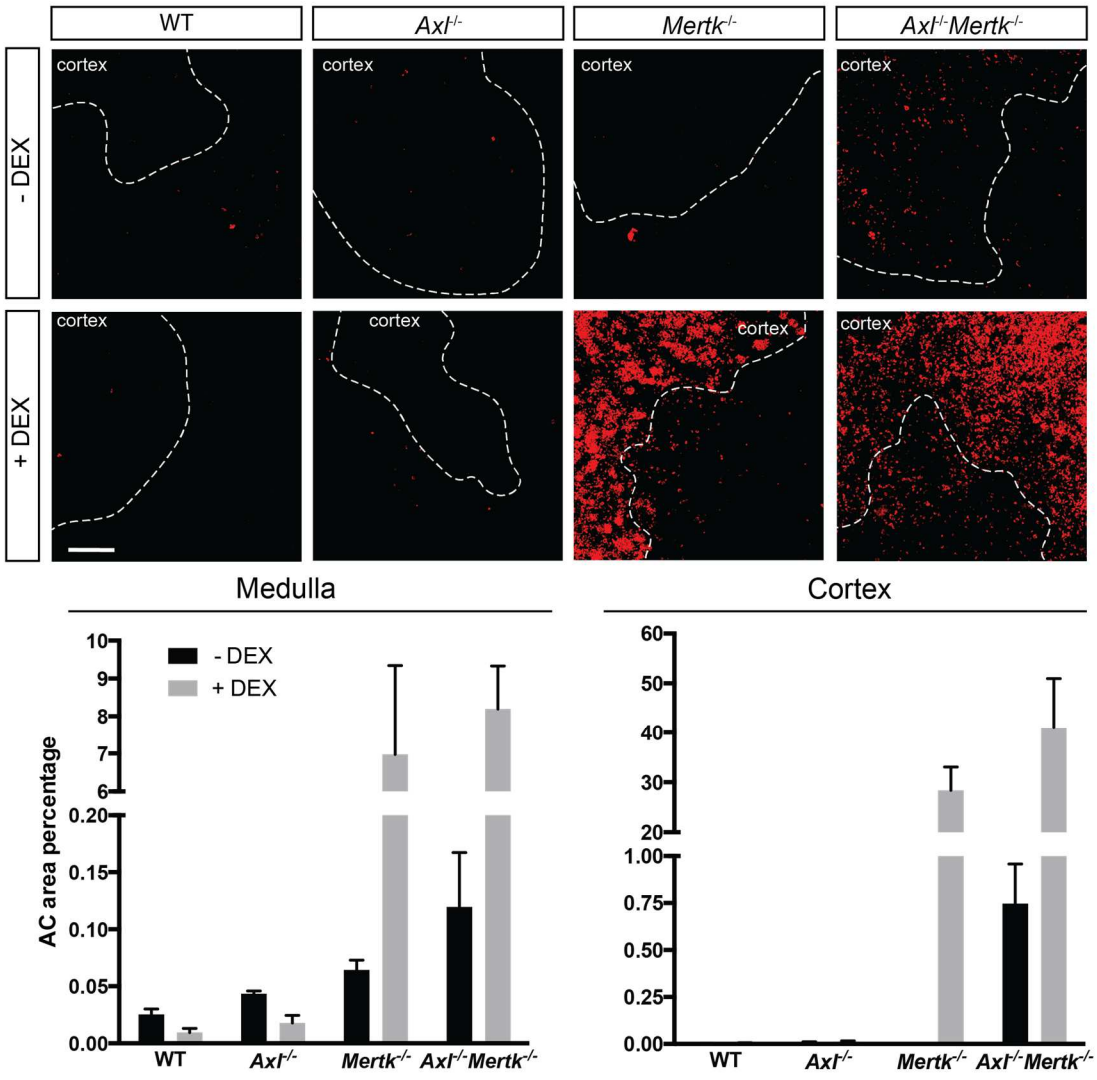

Figure 14. The Effects of Dexamethasone on Murine Thymus. 3-month-old female C57Bl/6 mice were injected with 0.2 mg/ 25 g DEX. Thymuses were harvested 24h after injection. – DEX denotes no injection and + DEX denotes DEX injection. Thymic sections were stained with CD86, cCasp3, and Hoechst. Representative images are shown. Scale bar,100 µm. AC area was measured with Image J and is presented below as a percentage of total region area. All error bars are SEM.

Dexamethasone Effects on Macrophages in the Thymus

When comparing the accumulation of apoptotic cells, in response to DEX injection, it was important to ensure that the stimuli did not change the

expression of TAM receptors in the thymus. Stimulation of murine bone marrow-derived macrophages (BMMΦ) with 100nM DEX for 24h eliminates expression of Axl and intensely upregulates expression of Mer (Zagorska et al., 2014). This has also been confirmed through Western blot analysis (data not shown). Immunohistochemistry was employed in order to see if DEX affects *in vivo* expression of Axl and Mer in the thymus. 12-week-old thymuses from DEX-injected and control WT were compared for Axl and Mer expression.

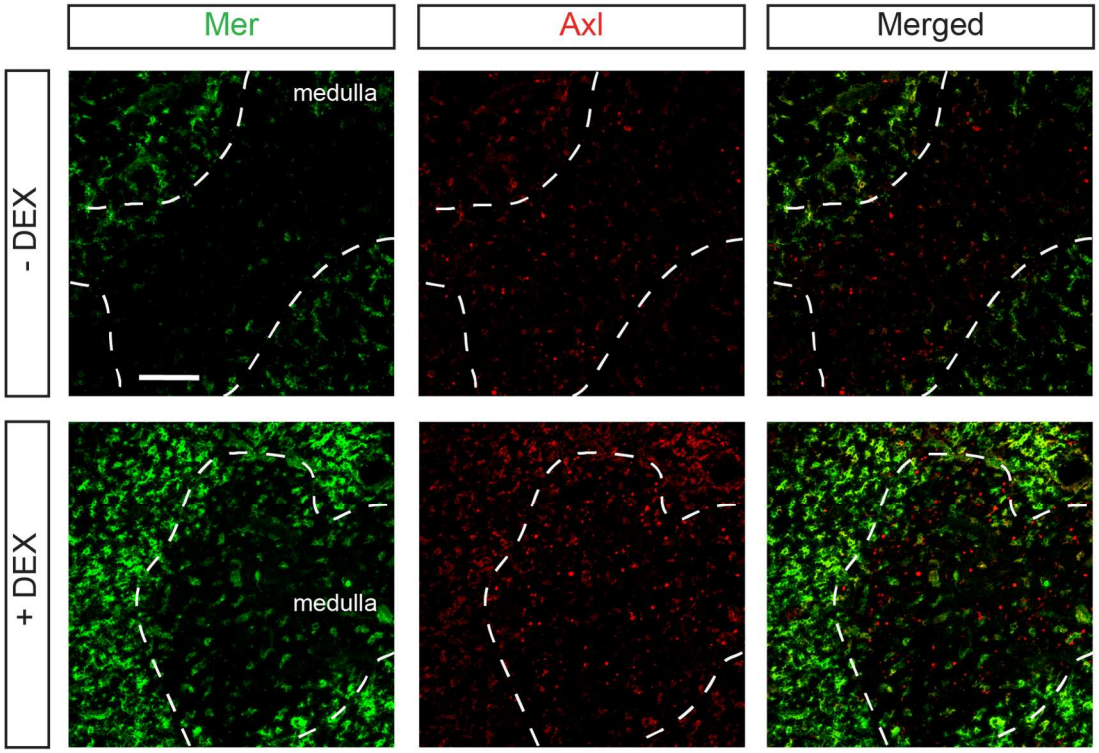

Figure 15. Effects of Dexamethasone on Axl and Mer Expression. 3-month-old, female, C57Bl/6 mice were injected with 0.2 mg/ 25 g DEX. Thymuses were harvested 24h after injection. Thymic sections were stained for Axl, Mer and Hoechst. Non-DEX treated thymus is shown above and DEX-treated thymus is shown below. The merged image of Axl and Mer expression is shown on the right. Scale bar, 100 μm.

Consistent with the BMMΦ results, there is significant increase in the level of Mer expression on the surface of macrophages in DEX-injected thymuses

(Figure 15). Interestingly, there is also a slight increase in the expression of Axl on macrophages in the cortex and medulla. This indicated that the AC clearance in mice injected with DEX might appear more Mer dependent due to the increased expression of Mer. Seeing that TAM expression was manipulated through DEX-injection, we further analyzed the AC accumulation in DEX and control WT thymus.

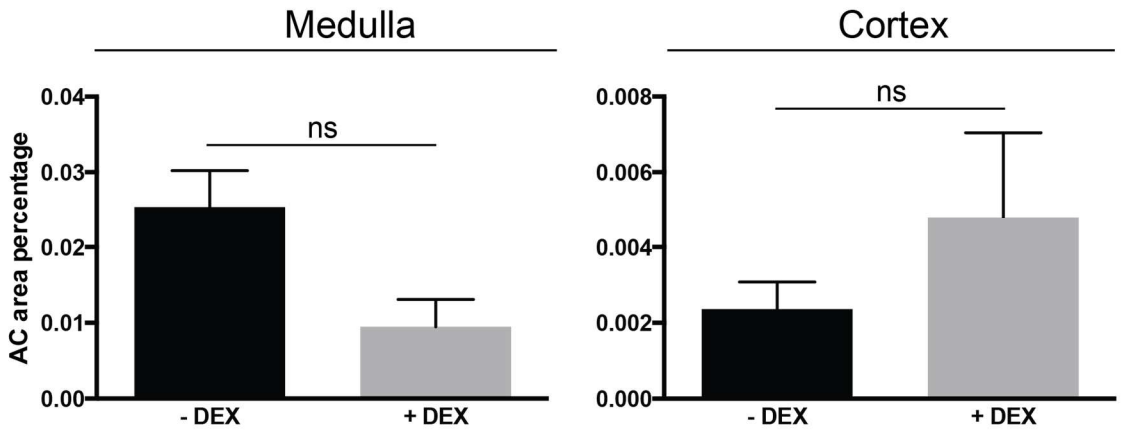

Figure 16. Dexamethasone Control for AC Accumulation. WT 3-month-old DEX-injected and control mice were analyzed for AC accumulation. ACs were analyzed by area percentage. ns = not significant. All error bars are SEM.

In the cortex and medulla, there is no significant change in the accumulation of apoptotic cells from DEX injection (Figure 16). However, it is interesting to note that there is a small decrease in the AC area with DEX injection in the medulla, which could result from increased Mer expression.

Morphological Analysis of Thymus

Another way to examine defects between the thymuses from TAM receptor knockout mice was to look at their morphological changes. While excising the thymus from the mice, *Axl*$^{-/-}$*Mertk*$^{-/-}$ and *Mertk*$^{-/-}$*Gas6*$^{-/-}$ thymuses appeared bigger in size compared to the single knockouts and WT thymus. To further quantify this visual difference, thymuses for 4-week-old mice were weighed and analyzed. To first determine if there mouse weight correlated with thymus weight, data points were plotted and analyzed on a scatter plot. Data points were pooled from various genotypes (Figure 17).

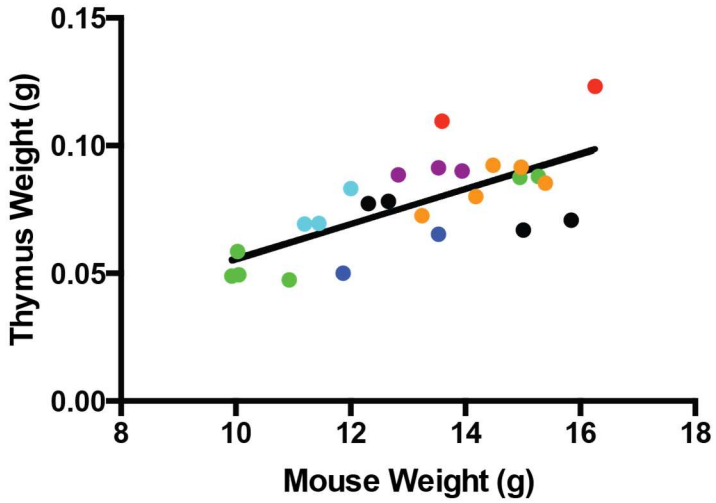

Figure 17. Correlation Between Mouse Weights and Thymic Weight. Thymuses from 4-week-old, female, C57Bl/6 mice were weighed immediately upon excision (n=25). Connective tissue and blood were removed before weighing. WT = Black; *Axl*$^{-/-}$ = Green; *Mertk*$^{-/-}$ = Blue; *Axl*$^{-/-}$*Mertk*$^{-/-}$ = Red; *Gas6*$^{-/-}$ = Orange; *Mertk*$^{-/-}$*Gas6*$^{-/-}$ = Purple; *Tyro3*$^{-/-}$ = Cyan. Pearson correlation was used for analysis. Pearson r = 0.6996.

Without taking genotype into effect, there was a strong positive correlation between mouse mass and thymus mass (R^2 = 0.4894). When compared to WT, there was no significant difference in thymic mass for *Axl*$^{-/-}$, *Mertk*$^{-/-}$, *Tyro3*$^{-/-}$, and

Gas6$^{-/-}$ mice. *Axl*$^{-/-}$*Mertk*$^{-/-}$ was the only genotype with a significant thymic weight percentage compared to WT (P=0.0337) (Figure 18).

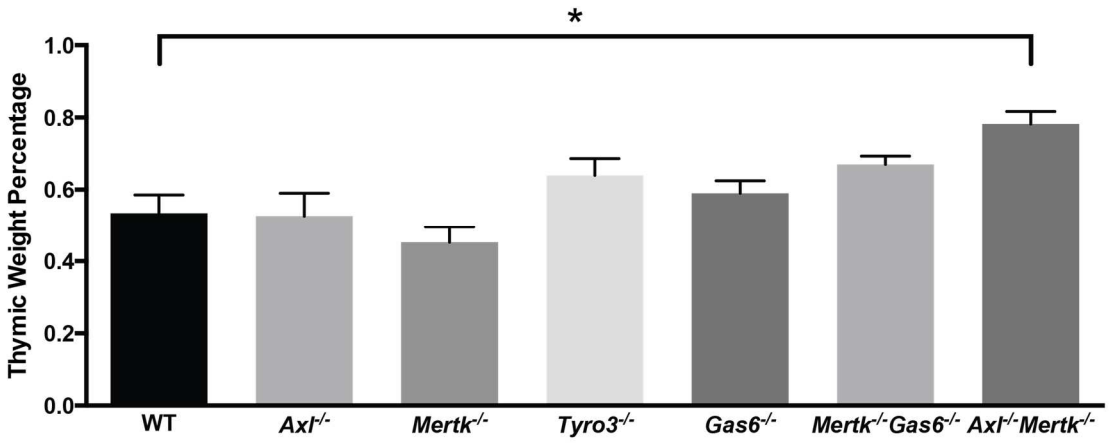

Figure 18. Thymic Weight as a Percentage of Body Weight. Thymus from 4-week-old, female, C57Bl/6 mice was massed. For all genotypes, n > 3 except for *Mertk*$^{-/-}$ and *Axl*$^{-/-}$*Mertk*$^{-/-}$, which were n = 2. All error bars are SEM.

Another possible defect between the genotypes is the ratio of the medulla to the cortex. To analyze medulla-cortex ratio, thymic slides were stained with Hematoxylin and Eosin in order to easily differentiate densely packed cortex regions from loosely packed medulla regions. In order to accurately analyze the ratio of cortex to medulla, three sections that were at least 100 μm apart were analyzed. This controlled for depth-dependent variations in the ratio of the two regions. For each section, total medulla and cortex area were measured. WT and *Axl*$^{-/-}$*Mertk*$^{-/-}$ mice were both analyzed at the 4 weeks of age. *Axl*$^{-/-}$*Mertk*$^{-/-}$ was chosen for analysis because this genotype accumulated the greatest number of ACs, and would thus probably present the most drastic ratio defect. For both WT and *Axl*$^{-/-}$*Mertk*$^{-/-}$, the percentage of cortex and medulla was 70% and 30%, respectively (Figure 19). Therefore, the accumulation of AC in *Axl*$^{-/-}$*Mertk*$^{-/-}$ did

not induce gross changes in *Axl*$^{-/-}$*Mertk*$^{-/-}$ thymus morphology at 4 weeks of age. It is still possible that there can be TAM-dependent morphological defects present during thymic involution in aged mice.

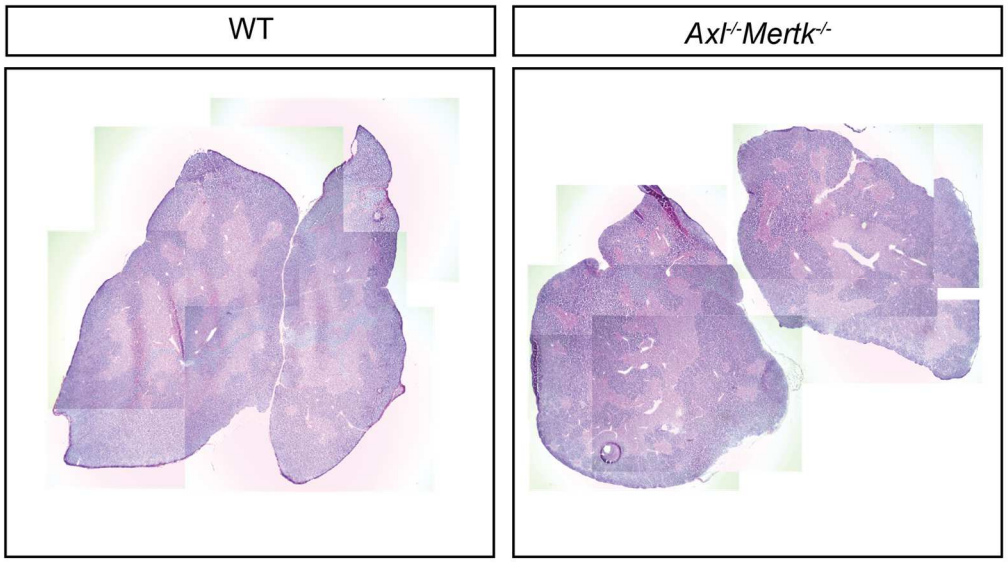

Figure 19. Hematoxylin & Eosin Staining of Medullary and Cortical Regions. Thymuses were stained with H&E (see methods) Slides were imaged at 4X magnification with a light microscope. Images were manually stitched. Entire medullary region was traced and the ratio of medulla to cortex was compared between genotypes.

DISCUSSION

Localization of Axl and Mer within the Thymus

The goal of our studies was to investigate the presence and the role of Axl and Mer within the thymus. We analyzed mouse thymus at different age to elucidate Axl and Mer function during thymic maturation and the thymic involution. Furthermore, we analyzed the function of these receptors at basal state as well as after the dexamethasone induced thymocyte death.

The purpose of the colocalization experiments was to determine if Axl and Mer were present within the thymus, and if present, which cells expressed these receptors. In previous studies, it was shown that Mer was expressed on thymic macrophages (Scott et al., 2001). Additionally, expression of Axl has been reported on thymic stromal cells (Rinke de Wit et al., 1996). From our Axl and Mer colocalization analysis, Axl was expressed on all Mer^+ cells but Mer was not expressed on all Axl^+ cells. Axl was chosen as the receptor to use in the colocalization assays because the species of the Mer antibody was the same species as many of our colocalization receptor antibodies. Our colocalization analysis revealed that Axl and Mer were primarily expressed on $F4/80^+CD68^+$ macrophages both in the medulla and cortex. CD169 and MARCO were two additional macrophage markers analyzed because they are expressed on immune cells within other lymphoid organs (Aichele et al., 2003). In other organs, CD169 is a marker for metallophilic macrophages. Their name is derived from

their affinity for silver and this population efficiently traps antigens from blood. In spleen and other tissues, MARCO is a marker for subsets of macrophages as well as splenic DCs. We showed for the first time that, in the thymus, both MARCO and CD169 stain Axl and Mer positive macrophages specifically in the cortex. Therefore these markers can be useful for discriminating between cortical and medullar macrophage populations.

Within the medulla, Axl but not Mer expression was also found to be present on DCs. For splenic DCs, it has been shown that Axl plays an important role in the continued clearance of ACs and is critical for cross-presentation of AC antigens to maturing T cells (Subramanian et al., 2014). It is feasible that Axl expression on thymic DCs could have similar role.

In summary we were able to resolve the location of Axl and Mer to cells responsible for exclusively phagocytosis (medullar and cortical macrophages) or phagocytosis and antigen presentation (medullar DCs). This finding matches the general understanding for the role of Axl and Mer as well as their localization on macrophages and other professional phagocytes. From this, we directed our focus on investigating the role of Axl and Mer in AC clearance in thymus.

Homeostatic Apoptotic Cell Clearance in Thymus

During thymic education the vast majority of thymocytes undergo apoptosis and only few percent are released to circulation. Most of the thymocytes (90%) fail to rearrange a functional TCR and die due to neglect.

Around 5% of developing T cells recognize self-antigens and those receive a strong pro-apoptotic signal and are eliminated by negative selection. Despite those vast numbers of cells dying daily, wild type thymus has relatively small number of accumulating AC as the apoptotic thymocytes are efficiently removed by cortical and medullar macrophages.

Our next goal was to understand Axl and Mer's ability to facilitate phagocytosis of apoptotic thymocytes by thymic macrophages. We used cleaved Caspase 3 (cCasp3) as a terminal marker of cellular apoptosis (Porter and Janicke, 1999). Accumulation of cCasp3-positive apoptotic cells usually indicates either increased apoptosis or a defect in clearance of apoptotic cells. Previous studies of TAM receptor KO cells showed that lack of TAM receptors do not affect the rate of apoptosis. Therefore the accumulation of ACs in *Axl*$^{-/-}$*Mertk*$^{-/-}$ thymus most likely results from a defective AC phagocytosis.

Our analysis showed that there is minimal AC accumulation in WT and in the single KOs mice. *Axl*$^{-/-}$ and *Mertk*$^{-/-}$ mice only showed a 2-fold increase in ACs specifically in the medulla. This however was different in the *Axl*$^{-/-}$*Mertk*$^{-/-}$ or *Mertk*$^{-/-}$*Gas6*$^{-/-}$. The absence of both receptors, or absence of Mer and Axl ligand, caused a drastic accumulation of ACs. This shows Axl and Mer can both facilitate the AC phagocytosis are redundant for the clearance process.

Most of the ACs observed in the WT thymus were localized in medulla and these are most probably single positive (SP) CD4 or CD8 thymocytes that are eliminated by medullar negative selection. The process for negative selection in the medulla occurs more slowly because the almost-mature thymocytes will only

die after repeatedly showing affinity to TSAs presented on mTECs and DCs. It is possible that we do not observe large numbers of AC in WT cortex because negative selection occurs mostly in the medulla while the cells dying from the neglect in cortex might actually be removed before they become cCasp3 positive. The AC accumulation within the *Axl*$^{-/-}$*Mertk*$^{-/-}$ is increased both in medulla and, to a greater extent, in cortex. This indicates that Axl and Mer facilitate the clearance of all cells eliminated during thymic education: the double negative (DN) cortical thymocytes that die due to neglect and the DP and SP thymocytes eliminated by negative selection in cortex and medulla, respectively. The observation that most of AC buildup in *Axl*$^{-/-}$*Mertk*$^{-/-}$ occurs in the cortex correspond to the fact that majority of thymocytes die in that region out of neglect. Their lack of clearance probably allows them to activate Caspase cascade.

The increased accumulation within the *Axl*$^{-/-}$*Mertk*$^{-/-}$ is of great interest because one of the phenotypes from *Axl*$^{-/-}$*Mertk*$^{-/-}$ mice is the development of autoimmune diseases. To further understand the effect of the *Axl*$^{-/-}$*Mertk*$^{-/-}$ within the thymus, it will be important to analyze if the inability to efficiently clear ACs leads to either an escape of immature or autoreactive thymocytes or a modulation in the thymocytes populations that exist in the periphery. The escape of immature thymocytes could connect the *Axl*$^{-/-}$*Mertk*$^{-/-}$ clearing deficiency with the autoimmune diseases that those mice develop. To understand the thymic disruption on peripheral T cell populations, flow cytometry analysis can be used to quantify T cell subpopulations. Immature T cells can be tested for Tdt (terminal deoxynucleotidyl transferase) (Hsu and Jaffe, 1985), which is an immature T cell

marker. This, in conjunction with globally conserved T cell markers could then test the immature T cell escape theory.

Alternatively, AC accumulation in thymus could result in changes of local environment in thymus that could also affect the properties of T cells released to the periphery. The change in local environment can arise from the unclear apoptotic cells becoming secondarily necrotic (Munoz et al., 2010). Secondarily necrotic cells undergo exposed autolysis, which would result in the accumulation of cellular components in the thymus. While H&E staining revealed no difference in the ratio of medulla to cortex in WT and *Axl*$^{-/-}$*Mertk*$^{-/-}$, individual zones relying on cytokine gradients could be disrupted. This would be especially detrimental in the medulla where the TCR is challenged for reactivity with autoantigens. An overburden in this region could decrease T cell interaction with mTECs. If an autoreactive T cell fails to interact with mTECs and APCs in medulla it could avoid apoptosis and exit the thymus fully matured. Measuring the area of these zones using specific markers would reveal if heavy AC accumulation changes the zonal ratios between genotypes.

Studying thymus also allowed us to compare the effects of Axl deletion to its ligand deletion. Gas6 is reported to be necessary and the only ligand for Axl activation. Interestingly, in 4-week-old mouse thymus, *Gas6*$^{-/-}$ accumulated fewer ACs than *Axl*$^{-/-}$, showing that the *Gas6*$^{-/-}$ was not as detrimental as the *Axl*$^{-/-}$. Some of the possible reasons for this could be: (a) the presence of alternative ligands specific for Axl within the thymus, (b) ligand-independent signaling of Axl e.g. via cross-dimerization with Mer, or (c) potential compensatory mechanism

due to the absence of Gas6 such as increased expression of ProS, Mer or other phagocytic receptors. The alternative ligand theory for Axl would allow for Axl and Mer to both function in the *Gas6*$^{-/-}$ and thus reduce the AC accumulation compared to the *Axl*$^{-/-}$. From the western blot analysis we confirm that there is no Tyro3 within the thymus, nor is there any compensatory upregulation of Axl or Mertk. Phenotypes in *Gas6*$^{-/-}$ and *Axl*$^{-/-}$ single KOs are subtle, thus to further investigate the role of Gas6 and Axl, *Mertk*$^{-/-}$*Gas6*$^{-/-}$ was compared to *Axl*$^{-/-}$*Mertk*$^{-/-}$. These two genotypes compare Axl and Gas6 deficiency in the Mer-null background, which removes the ability for Gas6 to function through Mer as well as the possibility for Axl-Mer cross dimerization. Both *Axl*$^{-/-}$*Mertk*$^{-/-}$ and *Mertk*$^{-/-}$ *Gas6*$^{-/-}$ thymus showed massive accumulation of ACs both in cortex and in medulla suggesting that indeed Gas6 is necessary for Axl function in the thymus. There was, however, a trend for higher AC numbers in AM DKO cortex as compared to *Mertk*$^{-/-}$*Gas6*$^{-/-}$ cortex. One possible explanation for lower accumulation in *Mertk*$^{-/-}$*Gas6*$^{-/-}$ would be through some residual Axl activity that could be either ligand independent or occurring through another ligand. It will be important to increase the sample size to see if difference between the two genotypes is truly significant.

Glucocorticoid Induced Changes in Thymocyte Apoptosis and Clearance

Beyond the basal AC accumulation, we also examined the Axl and Mer function in response to acute induction of thymocyte apoptosis. It has been

shown that dexamethasone causes specific death of $CD4^+CD8^+$ DP thymocytes (Purton et al., 2004; Tosa et al., 2003) as this subset is most sensitive to the corticosteroids. Dexamethasone treatment would increase the thymocyte apoptosis in the subcapsular region of the thymic cortex. It has previously been described that Mer plays a critical role in the clearance of apoptotic cells after dexamethasone injection (Scott et al., 2001). Consistent with that, we showed that in 12-week-old mice treated with DEX there is no AC accumulation in WT and *Axl*$^{-/-}$ thymus. In contrast, massive AC accumulation is present in the *Mertk*$^{-/-}$ and *Axl*$^{-/-}$*Mertk*$^{-/-}$ DEX-injected mice. The level of accumulation was so high that counting individual ACs was not feasible due to massive AC aggregation. This finding matched Scott and colleagues' observation that Mer was important for AC clearance after acute insult. However, it has been also published that dexamethasone treatment leads to both increased expression of Mer and decreased Axl expression in BMMΦ. This suggested that it was possible that dexamethasone treatment could modulate expression of Axl and Mer on thymic macrophages and therefore render the AC clearance more Mer-dependent. We checked Mer and Axl expression after DEX treatment and found that Mer was indeed highly upregulated in both the medulla and cortex. Axl expression was also upregulated but not to the same extent. The increased Mer expression after Dex injection can explain decreased AC numbers in medulla of Dex-injected WT and Axl KO mice. To further investigate this, Western blot analysis can be used to quantify the DEX-induced increase of Mer and Axl expression in thymus.

It is interesting to note that the AC accumulation is contained within the cortex with some in the medulla for either the *Mertk*$^{-/-}$ or *Axl*$^{-/-}$*Mertk*$^{-/-}$. While there is noticeable AC accumulation in medulla for *Mertk*$^{-/-}$ or *Axl*$^{-/-}$*Mertk*$^{-/-}$, the cortical AC area percentage is increased 4 and almost 6-fold, respectively. The confinement indicates that DEX specifically targets DP thymocytes. The medulla signal could either result from some death of SP thymocytes or be caused by drift due to the overburden in the cortex. The later is more probable due to unequal distribution of ACs in medulla with majority located at the CMJ.

To determine if clearance of acutely accumulated thymocytes is truly Mer-dependent and Axl-independent, it should be tested through another model that does not induce Mer expression. For example Gamma radiation could be used to specifically kill dividing cells in the thymus.

In summary, we reveal that both Axl and Mer play crucial roles in mature thymus by clearing ACs. Failure to clear these cells may be the reason for the escape of autoreactive T cells, which go on to spontaneously initiate broad-spectrum autoimmunity.

REFERENCES

Aichele, P., J. Zinke, L. Grode, R.A. Schwendener, S.H. Kaufmann, and P. Seiler. 2003. Macrophages of the splenic marginal zone are essential for trapping of blood-borne particulate antigen but dispensable for induction of specific T cell responses. *J Immunol* 171:1148-1155.

Angelillo-Scherrer, A., P. de Frutos, C. Aparicio, E. Melis, P. Savi, F. Lupu, J. Arnout, M. Dewerchin, M. Hoylaerts, J. Herbert, D. Collen, B. Dahlback, and P. Carmeliet. 2001. Deficiency or inhibition of Gas6 causes platelet dysfunction and protects mice against thrombosis. *Nat Med* 7:215-221.

Ardavin, C. 1997. Thymic dendritic cells. *Immunol Today* 18:350-361.

Bauer, T., A. Zagorska, J. Jurkin, N. Yasmin, R. Koffel, S. Richter, B. Gesslbauer, G. Lemke, and H. Strobl. 2012. Identification of Axl as a downstream effector of TGF-beta1 during Langerhans cell differentiation and epidermal homeostasis. *J Exp Med* 209:2033-2047.

Bernhard, C.A., C. Ried, S. Kochanek, and T. Brocker. 2015. CD169+ macrophages are sufficient for priming of CTLs with specificities left out by cross-priming dendritic cells. *Proc Natl Acad Sci U S A* 112:5461-5466.

Ciofani, M., G.C. Knowles, D.L. Wiest, H. von Boehmer, and J.C. Zuniga-Pflucker. 2006. Stage-specific and differential notch dependency at the alphabeta and gammadelta T lineage bifurcation. *Immunity* 25:105-116.

Damoiseaux, J.G., H. Yagita, K. Okumura, and P.J. van Breda Vriesman. 1998. Costimulatory molecules CD80 and CD86 in the rat; tissue distribution and expression by antigen-presenting cells. *J Leukoc Biol* 64:803-809.

Deftos, M.L., E. Huang, E.W. Ojala, K.A. Forbush, and M.J. Bevan. 2000. Notch1 signaling promotes the maturation of CD4 and CD8 SP thymocytes. *Immunity* 13:73-84.

Degermann, S., C.D. Surh, L.H. Glimcher, J. Sprent, and D. Lo. 1994. B7 expression on thymic medullary epithelium correlates with epithelium-mediated deletion of V beta 5+ thymocytes. *J Immunol* 152:3254-3263.

Derbinski, J., A. Schulte, B. Kyewski, and L. Klein. 2001. Promiscuous gene expression in medullary thymic epithelial cells mirrors the peripheral self. *Nat Immunol* 2:1032-1039.

Geissmann, F., S. Jung, and D.R. Littman. 2003. Blood monocytes consist of two principal subsets with distinct migratory properties. *Immunity* 19:71-82

Goldrath, A.W., and M.J. Bevan. 1999. Selecting and maintaining a diverse T-cell repertoire. *Nature* 402:255-262.

Haks, M.C., P. Krimpenfort, J.H. van den Brakel, and A.M. Kruisbeek. 1999. Pre-TCR signaling and inactivation of p53 induces crucial cell survival pathways in pre-T cells. *Immunity* 11:91-101.

Hirsch, S., J.M. Austyn, and S. Gordon. 1981. Expression of the macrophage-specific antigen F4/80 during differentiation of mouse bone marrow cells in culture. *J Exp Med* 154:713-725.

Hsu, S.M., and E.S. Jaffe. 1985. Phenotypic expression of T lymphocytes in thymus and peripheral lymphoid tissues. *Am J Pathol* 121:69-78.

Kang, Y.S., S. Yamazaki, T. Iyoda, M. Pack, S.A. Bruening, J.Y. Kim, K. Takahara, K. Inaba, R.M. Steinman, and C.G. Park. 2003. SIGN-R1, a novel C-type lectin expressed by marginal zone macrophages in spleen, mediates uptake of the polysaccharide dextran. *Int Immunol* 15:177-186.

Koppel, E.A., C.W. Wieland, V.C. van den Berg, M. Litjens, S. Florquin, Y. van Kooyk, T. van der Poll, and T.B. Geijtenbeek. 2005. Specific ICAM-3 grabbing nonintegrin-related 1 (SIGNR1) expressed by marginal zone macrophages is essential for defense against pulmonary Streptococcus pneumoniae infection. *Eur J Immunol* 35:2962-2969.

Kraal, G., L.J. van der Laan, O. Elomaa, and K. Tryggvason. 2000. The macrophage receptor MARCO. *Microbes Infect* 2:313-316.

Le Borgne, M., E. Ladi, I. Dzhagalov, P. Herzmark, Y.F. Liao, A.K. Chakraborty, and E.A. Robey. 2009. The impact of negative selection on thymocyte migration in the medulla. *Nat Immunol* 10:823-830.

Lemke, G., and T. Burstyn-Cohen. 2010. TAM receptors and the clearance of apoptotic cells. *Ann N Y Acad Sci* 1209:23-29.

Lemke, G., and C.V. Rothlin. 2008. Immunobiology of the TAM receptors. *Nat Rev Immunol* 8:327-336.

Lew, E.D., J. Oh, P.G. Burrola, I. Lax, A. Zagorska, P.G. Traves, J. Schlessinger, and G. Lemke. 2014. Differential TAM receptor-ligand-phospholipid interactions delimit differential TAM bioactivities. *Elife* 3:

Lu, Q., M. Gore, Q. Zhang, T. Camenisch, S. Boast, F. Casagranda, C. Lai, M.K. Skinner, R. Klein, G.K. Matsushima, H.S. Earp, S.P. Goff, and G. Lemke. 1999. Tyro-3

family receptors are essential regulators of mammalian spermatogenesis. *Nature* 398:723-728.

Mandal, M., C. Borowski, T. Palomero, A.A. Ferrando, P. Oberdoerffer, F. Meng, A. Ruiz-Vela, M. Ciofani, J.C. Zuniga-Pflucker, I. Screpanti, A.T. Look, S.J. Korsmeyer, K. Rajewsky, H. von Boehmer, and I. Aifantis. 2005. The BCL2A1 gene as a pre-T cell receptor-induced regulator of thymocyte survival. *J Exp Med* 201:603-614.

Martinez-Pomares, L., and S. Gordon. 2012. CD169+ macrophages at the crossroads of antigen presentation. *Trends Immunol* 33:66-70.

McCaughtry, T.M., M.S. Wilken, and K.A. Hogquist. 2007. Thymic emigration revisited. *J Exp Med* 204:2513-2520.

Morris, L., C.F. Graham, and S. Gordon. 1991. Macrophages in haemopoietic and other tissues of the developing mouse detected by the monoclonal antibody F4/80. *Development* 112:517-526.

Munoz, L.E., K. Lauber, M. Schiller, A.A. Manfredi, and M. Herrmann. 2010. The role of defective clearance of apoptotic cells in systemic autoimmunity. *Nat Rev Rheumatol* 6:280-289.

Murray, P.J., and T.A. Wynn. 2011. Protective and pathogenic functions of macrophage subsets. *Nat Rev Immunol* 11:723-737.

Palmer, E. 2003. Negative selection--clearing out the bad apples from the T-cell repertoire. *Nat Rev Immunol* 3:383-391.

Petrie, H.T., and J.C. Zuniga-Pflucker. 2007. Zoned out: functional mapping of stromal signaling microenvironments in the thymus. *Annu Rev Immunol* 25:649-679.

Pierce, A.M., and A.K. Keating. 2014. TAM receptor tyrosine kinases: expression, disease and oncogenesis in the central nervous system. *Brain Res* 1542:206-220.

Porter, A.G., and R.U. Janicke. 1999. Emerging roles of caspase-3 in apoptosis. *Cell Death Differ* 6:99-104.

Purton, J.F., J.A. Monk, D.R. Liddicoat, K. Kyparissoudis, S. Sakkal, S.J. Richardson, D.I. Godfrey, and T.J. Cole. 2004. Expression of the glucocorticoid receptor from the 1A promoter correlates with T lymphocyte sensitivity to glucocorticoid-induced cell death. *J Immunol* 173:3816-3824.

Ravichandran, K.S. 2010. Find-me and eat-me signals in apoptotic cell clearance: progress and conundrums. *J Exp Med* 207:1807-1817.

Riedinger, M., K. Karjalainen, and T. Brocker. 1997. Targeted expression of MHC class II genes to dendritic cells in vivo. *Immunol Lett* 57:155-158.

Rinke de Wit, T.F., D.J. Izon, C. Revilla, M. Oosterwegel, A.Q. Bakker, W. van Ewijk, and A.M. Kruisbeek. 1996. Expression of tyrosine kinase gene in mouse thymic stromal cells. *Int Immunol* 8:1787-1795.

Robey, E., and B.J. Fowlkes. 1994. Selective events in T cell development. *Annu Rev Immunol* 12:675-705.

Scott, R.S., E.J. McMahon, S.M. Pop, E.A. Reap, R. Caricchio, P.L. Cohen, H.S. Earp, and G.K. Matsushima. 2001. Phagocytosis and clearance of apoptotic cells is mediated by MER. *Nature* 411:207-211.

Segawa, K., and S. Nagata. 2015. An Apoptotic 'Eat Me' Signal: Phosphatidylserine Exposure. *Trends Cell Biol* 25:639-650.

Seitz, H.M., T.D. Camenisch, G. Lemke, H.S. Earp, and G.K. Matsushima. 2007. Macrophages and dendritic cells use different Axl/Mertk/Tyro3 receptors in clearance of apoptotic cells. *J Immunol* 178:5635-5642.

Speiser, D.E., R.K. Lees, H. Hengartner, R.M. Zinkernagel, and H.R. MacDonald. 1989. Positive and negative selection of T cell receptor V beta domains controlled by distinct cell populations in the thymus. *J Exp Med* 170:2165-2170.

Spits, H. 2002. Development of alphabeta T cells in the human thymus. *Nat Rev Immunol* 2:760-772.

Stitt, T.N., G. Conn, M. Gore, C. Lai, J. Bruno, C. Radziejewski, K. Mattsson, J. Fisher, D.R. Gies, P.F. Jones, and et al. 1995. The anticoagulation factor protein S and its relative, Gas6, are ligands for the Tyro 3/Axl family of receptor tyrosine kinases. *Cell* 80:661-670.

Subramanian, M., C.D. Hayes, J.J. Thome, E. Thorp, G.K. Matsushima, J. Herz, D.L. Farber, K. Liu, M. Lakshmana, and I. Tabas. 2014. An AXL/LRP-1/RANBP9 complex mediates DC efferocytosis and antigen cross-presentation in vivo. *J Clin Invest* 124:1296-1308.

Surh, C.D., and J. Sprent. 1994. T-cell apoptosis detected in situ during positive and negative selection in the thymus. *Nature* 372:100-103.

Szondy, Z., E. Garabuczi, K. Toth, B. Kiss, and K. Koroskenyi. 2012. Thymocyte death by neglect: contribution of engulfing macrophages. *Eur J Immunol* 42:1662-1667.

Takahama, Y. 2006. Journey through the thymus: stromal guides for T-cell development and selection. *Nat Rev Immunol* 6:127-135.

Tosa, N., M. Murakami, W.Y. Jia, M. Yokoyama, T. Masunaga, C. Iwabuchi, M. Inobe, K. Iwabuchi, T. Miyazaki, K. Onoe, M. Iwata, and T. Uede. 2003. Critical function of T cell death-associated gene 8 in glucocorticoid-induced thymocyte apoptosis. *Int Immunol* 15:741-749.

van Meer, G., D.R. Voelker, and G.W. Feigenson. 2008. Membrane lipids: where they are and how they behave. *Nat Rev Mol Cell Biol* 9:112-124.

Varnum, B.C., C. Young, G. Elliott, A. Garcia, T.D. Bartley, Y.W. Fridell, R.W. Hunt, G. Trail, C. Clogston, R.J. Toso, and et al. 1995. Axl receptor tyrosine kinase stimulated by the vitamin K-dependent protein encoded by growth-arrest-specific gene 6. *Nature* 373:623-626.

Vollmer, J., H.U. Weltzien, K. Gamerdinger, S. Lang, Y. Choleva, and C. Moulon. 2000. Antigen contacts by Ni-reactive TCR: typical alphass chain cooperation versus alpha chain-dominated specificity. *Int Immunol* 12:1723-1731.

Weinreich, M.A., S.C. Jameson, and K.A. Hogquist. 2011. Postselection thymocyte maturation and emigration are independent of IL-7 and ERK5. *J Immunol* 186:1343-1347.

Witt, C.M., S. Raychaudhuri, B. Schaefer, A.K. Chakraborty, and E.A. Robey. 2005. Directed migration of positively selected thymocytes visualized in real time. *PLoS Biol* 3:e160.

Wood, G.W. 1985. Macrophages in the thymus. *Surv Immunol Res* 4:179-191.

Wu, L., and K. Shortman. 2005. Heterogeneity of thymic dendritic cells. *Semin Immunol* 17:304-312.

Zagorska, A., P.G. Traves, E.D. Lew, I. Dransfield, and G. Lemke. 2014. Diversification of TAM receptor tyrosine kinase function. *Nat Immunol* 15:920-928.

American Cancer Society. (2015). Retrieved from http://www.cancer.org/research/cancerfactsstatistics/cancerfactsfigures2015/

National Institute of Health. (2015). Retrieved from http://www.niaid.nih.gov/topics/autoimmune/pages/default.aspx